YOKOHAMA NATIONAL UNIVERSITY

PhD dissertation

Evaluation of vehicle dynamic load effects on existing bridges considering traffic flow and surface roughness condition

Author:

HO THI HOAI

Supervisors:

Prof. Hitoshi YAMADA

Ass. Prof. Mayuko NISHIO

A dissertation submitted in partial fulfilment of the requirements for the degree of Doctor of philosophy (in Engineering) in the Department of Urban Innovation

September 05th, 2019

ABSTRACT

The variation of vehicle types, speeds, passing orders in traffic flow, and roughness conditions fluctuate the vehicle dynamic load effect in existing bridges. This thesis proposed a numerical calculation scheme to evaluate the bridge dynamic responses and dynamic impact factor considering traffic flow and random and local surface roughness condition.

In this study, measured traffic data, measured bridge response, roughness profile, and FE model of the target structure are required as the input for implementing the numerical scheme. The measured acceleration is used for validating the FE model of target bridge and numerical scheme result. The numbers of each vehicle type passing through bridge at certain time interval are collected for traffic modelling. The fluctuation of total load of car and truck considering uncertainty in suspension system, different speeds, and roughness condition are calculated in vehicle roughness interaction simulation. From extracted traffic patterns and statistical value of total vehicular load, traffic flow with random passing orders of vehicles is constructed as transient time history loading function assigned on the deck nodes of the target bridge FE model. The validity of the calculation scheme is verified by applying it to a target bridge. The parametric study was then conducted to investigate the effects of traffic flow characteristics and random surface roughness conditions on the bridge dynamic responses. It was shown that the RMS acceleration depends on the truck ratio and vehicle velocity meanwhile maximum value was influenced by vehicle speed, passing orders, and the surface roughness condition. Effect of local surface damage on bridge dynamic response is also investigated by using the proposed numerical scheme. The increment of the dynamic effect of traffic vehicles on bridges is indicated by the ratio α between RMS acceleration at condition *i* and good surface roughness condition. The relationship between IM and α in two existing bridges is constructed. The scheme proposed dynamic impact factor of given traffic flow and local surface damage condition which can be used for calculating rating factor of existing bridges.

In this thesis, a calculation scheme was introduced to evaluate vehicle dynamic load effect of existing bridges with the given dynamic monitoring data, traffic flow, and surface roughness condition. The study also proposed a dynamic ratio α to calculate dynamic impact factor of bridge under traffic flow and local surface damage condition which could be used for evaluating rating factor in existing bridge condition assessment.

ACKNOWLEDGMENTS

Immeasurable appreciation and deepest gratitude for the help and supports are expressed to the following individuals and organization who/ which have contributed to make this study possible:

To **Assoc. Prof. Mayuko Nishio and Prof. Hitoshi Yamada,** for their patience, expertise and experience during three years of my research. I have been amazingly fortunate to have advisors like them to give me the freedom to explore on my own idea and help me overcome many difficulties, both personal and professional, throughout the duration of my study. I am also thankful to them for their untiring guidance and great comments in my research progress.

I would like to say thanks to **Prof. Yozo Fujino, Prof. Hiroshi Katsuchi, Prof. Dionysius M Siringoringo, Prof. Kimitoshi Hayano** and **Assoc. Prof. Hiroshi Tamura** for serving as the committee members of my PhD study. All their valuable comments, suggestions, and support significantly contribute for the accomplishment of this study.

To **HEIWA NAKAJIMA foundation** for the granting project of bridge and surface roughness measurement in Vietnam. In this project, I would like to say thank to the great support from **Dr. Hien Van Le** and **Assoc. Prof. Huong Ho Lan**, University of Transport and Communications.

I also appreciated the continuous support of our laboratory secretary, **Mrs. Sakai**, who always provides the great help during the past 5 years of my study in YNU.

To **Dr. Kim Hae Young** and **all my fellow laboratory members,** for the guidance and cooperation during research discussions and learning process.

To **Ministry of Education, Culture, Sports, Science and Technology (MEXT), Japan,** for their financial support granted through my studies.

And finally, to **my big family** for their encouragement and endless love.

LIST OF FIGURES

LIST OF TABLES

NOMENCLATURE

ADTT : Average Daily Truck Traffic

c_s : Suspension damping

COV_{ck} : Selected coefficient of variation of total load of car at sample #k

COV_{tk} : Coefficient of variation of total load of truck at sample #k

D_c : Concrete density

DOF : Degree of freedom

$\triangle n$: Frequency band

D_s : Steel density

Fig. : Figure

$g_d(n)$: Power spectrum density function of road class at spatial frequency n

$g_d(n_0)$: Power spectrum density function of road class at spatial frequency

$h(x)$: Road surface profile at location x

i : Number of frequency steps

IM : Dynamic impact factor

IRI : Turbulent Intensity

k : Sample number in calculated mean and COV of total load

k_s : Suspension stiffness

k_t : Tire stiffness

K : Traffic density

m_s : Sprung mass

m_u : Un-sprung mass

n_0 : Reference spatial frequency

n_1 : Lower cut-off spatial frequency

n_2 : Higher cut-off spatial frequency

N : Number of frequency band

N_{tr} : Traffic volume

φ_i : Random phase angle of surface profile

ρ_c : Poisson ratio of concrete

ρ_s : Poisson ratio of steel

$\tilde{P}_{cijk}$: Varying load of car #*i* at node #*j* from mean and COV at sample #*k*

P_{ck} : Selected mean of total load of car at sample #*k*

P_{tk} : Selected mean of total load of truck at sample #*k*

$\tilde{P}_{tijk}$: Varying load of truck #*i* at node #*j* from mean and COV at sample #*k*

P_{dyn} : Dynamic load

P_{total} : Total load

$R_{dynamic}$: Dynamic effect

RMS : Root mean square

R_{static} : Static effect

V : Average velocity of traffic flow

WIM : Weight in motion

x : Location of quarter car model on surface profile

y_1 : Sprung mass displacement

y_2 : Un-sprung mass displacement

$\dot{y}_1$: Sprung mass velocity

$\dot{y}_2$: Un-sprung mass velocity

γ_c : Young modulus of concrete

γ_s : Young modulus of steel

TABLE OF CONTENTS

Chapter 1

1. INTRODUCTION

The evaluation of dynamic responses in associated with moving traffic and surface irregularity is an inevitable task of bridge maintenance procedure. The surface condition of existing bridges damaged severely due to temperature, heavy vehicles, and inadequate construction technology. High temperature during summer time has harden and melted the deck surface of the bridges. The cumulative effect of vehicular load commuting on the bridge, especially heavy trucks and trailers lead to the permanent deformation on bridge surface and the damage on bridge components. The increase in the number of vehicles and their weight on the bridge accelerated the deflects on bridge pavement and vice versa. The problem of evaluating the vehicle dynamic effect on existing bridges considering the traffic flow and roughness condition is required for the maintenance work of bridge during service stage.

1.1 Introduction

When vehicles pass through the bridge, the vehicular axle load is oscillated due to the interaction of vehicle suspension system, bridge and surface roughness. As a result, the induced dynamic loading causes the fluctuation of bridge dynamic response. To assure the bridge safety under the dynamic effect of traffic flow, the bridge specifications provide conservative values of the dynamic impact factor (IM) in design stage. These values of IM can be measured from field test or by the analytical simulation. From the result of the tests and simulation, the code provisions specify IM as a simple formula of a bridge parameter or traffic loading.

(a) Shoving (b) Transverse crack

Figure 1.1: Surface damage on bridge deck

AASHTO LRFD manual for bridge design sets the single IM value of and 0.15 for fatigue and fracture and 0.33 for the rest of limit states [1]. These values of dynamic impact factor was statistically calculated from a single truck and two trucks travelling on average surface condition in ISO class [2]. Therefore, as the road surface deteriorated, the value of IM may not practically applicable. For load rating of existing bridges, AASHTO LRFR sets the value of IM differently in different load rating procedures [3]. Base on the purpose of load rating and the condition of the bridge, the procedure of load rating is classified into three categories. They are design load rating, permit load rating, and legal load rating. The design load rating includes the inventory level and operating level which apply the same IM as specified in LRFD specification. Since the bridge surface is deteriorated and the live load of traffic on bridge changes in service time, the value of IM and live load factor on bridge for legal and permit load rating is calibrated. LRFR code reduces the value of impact factor to 0.1 and 0.2 in short span bridges with good surface roughness condition and minor deviation in existing

bridges. If vehicles run with crawling speed, the IM in permit load rating is set to be zero. Table 1.1 present the dynamic impact factor is selected for LRFR codes according to the condition of surface roughness. It should be note that all load rating procedures apply the single IM to calculate load rating factor. Other countries calculate the impact factor as a function of span length [4], [5], bridge fundamental frequency [6], [7] or typical loading model [8], [9], [10]. Deng and Cai [11], [12] found that the conservative values of IM in bridge specifications are underestimate in bad surface condition. Fig. 1.2 presents the dynamic impact factor in Canadian code as a function of bridge fundamental frequencies [6]. Fig. 1.3 presents the IM based on different roughness. It could be concluded that when the bridge surface roughness is deteriorated and traffic flow increases, the evaluation of bridge dynamic responses and IM in existing bridges are required.

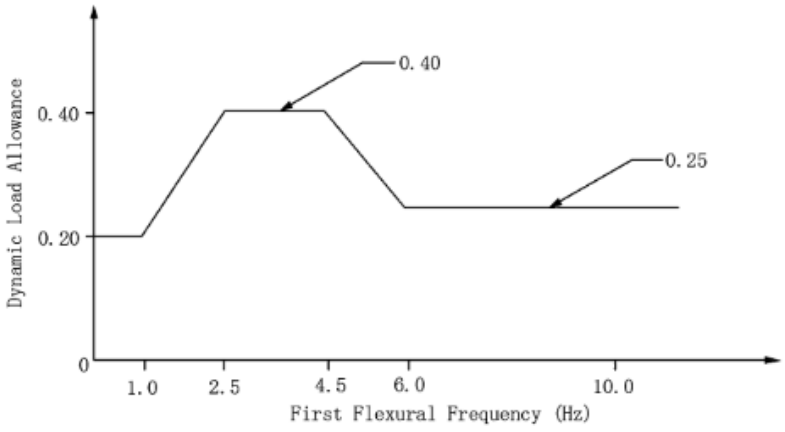

Figure 1.2: Dynamic impact factor in Canadian code [6]

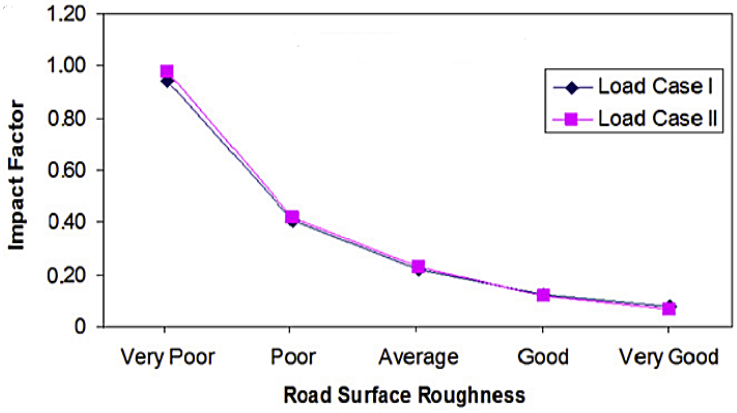

Figure 1.3: Dynamic impact factor of bridge under different surface roughness condition [11]

Table 1.1: IM in AASHTO LRFR Code for Legal rating

Riding surface condition	**IM**
Smooth riding surface at approaches, bridge deck and expansion join	0.1
Minor surface deviations or depressions	0.2
Significant deviations in riding surface at approaches, bridge deck, and expansion joints	0.33

Previous studies found that the road surface roughness could significantly vary the dynamic axle load of vehicle. According to the work of Mitchell and Gyenes [13] the peak of vehicular axle loads can equal to two times of static force and their root mean square (RMS) could reach to 30% of the static value. Fig. 1.4 plot the simulated dynamic load of vehicle pass through the bridge with different roughness condition in the work of Deng et al [14]. The result showed that the more damage the roughness profile is, the higher peak of vehicular load of vehicle. Hahn [15] suggested that when the same type of vehicle runs over the pavement at the same speed, the peak dynamic tire load always occurs within a typical section with local damage. This spatial repeatability phenomenon results in the increment of surface deterioration level from 1.5 to 12 times [16] and fluctuates the bridge dynamic response. According to Potter et al [17], the road roughness irregularity is the main cause of the fluctuation in dynamic tyre force and the suspension oscillation of vehicle. Pesterev et al [18] indicated that "dynamic contact forces arising when a vehicle passes typical road surface irregularities are considerably greater than those caused by coupled bridge–vehicle vibration in the case of ideally smooth road surface". The location of damage roughness on bridge also increases the axial load of vehicle and dynamic effect on bridges. Michaltsos [19] found that the irregularities at the beginning, the quarter, and the middle of bridge span cause the most unfavourable responses. The work of Obrien [20] also pointed out that the locations of bump on bridge influence on the bridge moment. Fig. 1.5 plots the normalize moment of bridge deck with variable speeds based on the relative location of unit ramp on bridge length in the study. The figure showed that the bump before the mid span length of the bridge 0.5 L has high influence on bridge response meanwhile the irregularity after that makes no contribution on the fluctuation of bridge moment. It can be

concluded that the local damage of surface roughness could increase or cancel out the dynamic load of vehicle and response of the bridge.

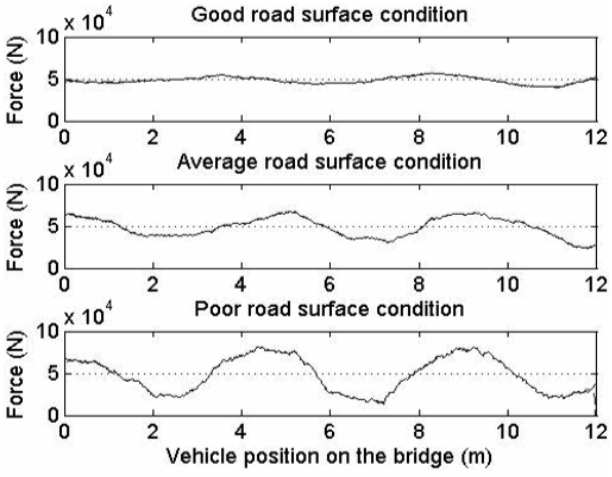

Figure 1.4: Dynamic load of vehicle under different roughness conditions [14]

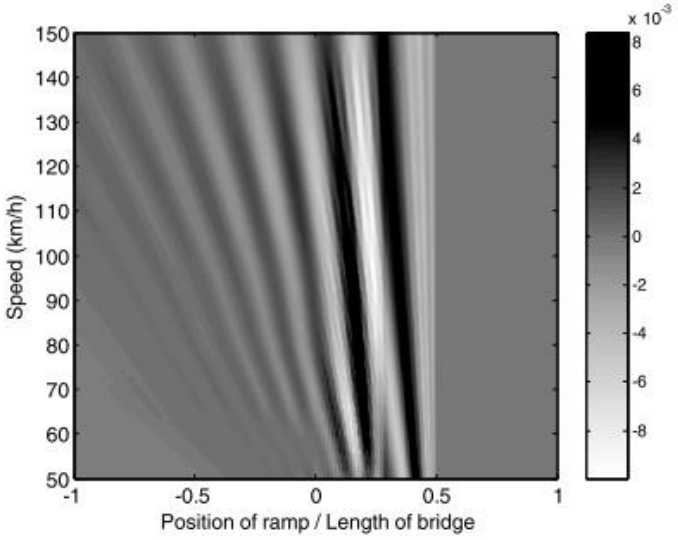

Figure 1.5: Normalized moment of bridge with the postion of unit ramp [20]

The study on evaluating the dynamic response of bridge under moving traffic vehicles is generally defined as vehicle bridge interaction (VBI). This problem has been studied and developed for years, starting from the pioneer work on rail way bridge of Willis et al [21] in nineteen century. The results of VBI study depend on variable of criteria such as traffic vehicle, bridge properties, and surface roughness condition. The analytical simulation of VBI problem requires the vehicle, bridge, and road surface modelling. Base on the desired accuracy level of the simulation, the complexity of vehicle and bridge modelling are different. The moving

vehicle could be modelled as moving force, moving mass, or sprung mass model. The moving load method was applied on in the early stage of VBI problem [22-26]. Although it is the simplest and convenient approach, the accuracy level is not high in case the heavy vehicles pass through the bridge. The moving mass model [27-31] also considers the effect of the vehicle mass, however, the bouncing effect of vehicle from bridge is not included. When the bridge has damage surface roughness, it is necessary to consider the interaction between vehicle and bridge. Therefore, the sprung mass model [32-37] could yield the most accuracy in VBI problem since it represents both the mass and suspension characteristic of vehicles. A lot of effort has been made to include the complexity of sprung mass model by increasing the number of DOF of the vehicle system. Recently, the development of computational technology enables the construction of detail suspension model of vehicle. These models have successfully identified the varying contact force between vehicle and bridge in space and time [11; 38; 39]. The detail multiple degree of freedom model of vehicle could represent the dynamic properties of vehicle suspension and tire characteristics. Meanwhile the discretised simple Euler Bernoulli beam model [40; 41] to complex 3D bridge model [11; 39; 42] could be conveniently constructed through the available commercial FE packages software. The surface roughness profile can be practically measured by the roughness profiler or commonly simulated as a random signal from power spectrum density (PSD) value in ISO classification [43]. The equation of motions of both bridge and vehicle are solved separately by iterative process [35; 44; 45] or by coupling two systems via interaction force between vehicle roughness and bridge [46-48]. The first method could gain very high accuracy; however, it requires more computational cost. The coupled approach uses the Newmark beta or Runge-Kutta method to solve the assembled equation of motions of vehicle bridge interaction system. It should be noted that the current VBI studies only calculated bridge dynamic response and IM due to a single or couple vehicles, however, the effect of random traffic condition has not yet fully investigated. In practice, the multi present of different vehicles types in random traffic flow could cause the variation of dynamic axle impact load fluctuations in space and time. The dynamic responses of bridge and IM will be amplified due to the random combination of traffic patterns (types, speed, passing order, etc…) and surface roughness condition (random and local damage) rather than from single or a couple of vehicle and roughness condition. The calculated dynamic vehicle load effect considering both effect of traffic flow and roughness relate to the change of IM in existing bridges.

Currently, weight in motion (WIM) data is used for characterizing the effect traffic patterns on roads and bridges. WIM station has been widely applied on highway to weight the

vehicles passing through the specific sites. It provides the data of vehicle types, speed, gross weight of each axle, axle spacing, and the distribution of heavy vehicles in traffic. WIM data is collected in months or years to provide the statistical information of traffic on sites and restrict the overweight vehicles which cause the pavement damage and excessive bridge vibration. It is also used to calibrate of design load and assess the fatigue of existing bridges. The WIM data variates depend on the location of test sites and requires a lot of test to compare the accuracy of technology of WIM method. In 1970s, of the bridge WIM technique was first applied on bridge by attaching the sensors on girder and the pavement to collect the weight, speed, axle spacing of traffic vehicles on bridge [49]. The measured strain data will be used to calculate the gross weight of passing vehicle by applying the influence line technique [50; 51]. The specification of WIM system and techniques can be found in ASTM-1318 for North America and COST323 for European countries. The improvement of the accuracy of bridge WIM system is recently developed in BridgeMon project [52]. It considers the vibration of the bridge, vehicle speed, temperature calibration, and improves the axle detection technique of vehicle. From the measured traffic flow characteristics of WIM, many studies simulated the traffic flow via simple random processes [53],[54] and Monte Carlo simulation of traffic parameters [55], [56], [57],[58]. The studies used the collected state WIM data to evaluate the expected maximum load effect on bridge. The live load factor in AASHTO LRFD is also calculated based on the provided Average Daily Truck Traffic (ADTT). The WIM data is often applied in term of statistical information, not for constructing the random of traffic flow on bridge. Only little effort used VBI to estimate the amplified contact force between vehicle on bridge and considered variation of vehicle types, speed, roughness via cellular automaton model for traffic flow [59], [60]. In previous literatures, most of researches on traffic scenario simulation collected vehicle gross weight data from WIM for statistic approach. The collected WIM data could be used to construct the traffic flow on bridge. The built-in traffic flow in combine with the roughness condition could be applied for evaluating bridge dynamic response and IM in existing bridges.

The aforementioned literature review includes information about the studies on effect of surface roughness on dynamic vehicle load, the current researches of VBI problem with their relation on bridge dynamic response and IM applied in LRFD and LRFR specification, and WIM technology application in characterizing live load effect. The previous VBI techniques precisely evaluated the dynamic effect of vehicle characteristics, vehicle speed, and surface roughness condition on the bridge with the consideration of a passing vehicle or a coupled

vehicle. In most of VBI research, the effect of random traffic flow patterns is not yet fully investigated. Meanwhile, WIM data can characterize traffic flow and it is statistically applied for estimating the expected maximum live load effect on bridge. The combine effect of traffic flow patterns and roughness condition, especially with local should be further studied. It is necessary to construct an approach for considering both traffic flow and roughness condition to evaluate vehicle dynamic load effect relating to IM in existing bridges.

The random dynamic load of vehicle is originated from the variation of vehicle types, vehicle properties, passing orders, speeds, and surface roughness condition of the bridges. The random variations of dynamic vehicular loads on the bridges is the main cause of the increment of dynamic responses, especially in existing bridges. Moreover, a lot of previous studies only constructed 1D or 2D correlated roughness without considering local damage surface in bridge deck. It should be noted that the local roughness damage of bridge will influence on the dynamic impact factor of passing traffic vehicles. Therefore, a method which incorporates the combination effect of traffic flow patterns and local roughness damage is required for bridge condition evaluation. The collected traffic data could be used for constructing the random traffic flow on bridge.

1.2 Purpose

This study aims provide an approach to estimate dynamic impact factor IM in existing bridge caused by the random and local roughness damage and current traffic condition with variation patterns: vehicle types, vehicle properties, speeds, passing order, and traffic volume. The traffic flow is constructed from the collected number of vehicles passing though the bridge in specific interval. Each vehicle is represented by transient forcing function. The traffic flow is considered as time history forcing function of vehicles assigned at each discretized deck node of bridge FE model. Consider that the stiffness of vehicle is much smaller than that of bridge, the interaction of vehicle and bridge is small in compare with effect of surface condition. Then, the random effect of different surface damage on traffic vehicles is facilitated via the fluctuation level of the built-in forcing's amplitude. As compared with previous studies, this research considers the effect of traffic flow patterns and roughness effect, uncertainty of vehicle parameters, random and local damage in time history analysis. The calculated dynamic responses of bridge under the variation of traffic volume, vehicle type, vehicle properties, speed,

vehicle passing order and the roughness condition indicates the change of IM could provide useful information for bridge condition evaluation and load rating in LRFR.

1.3 Outline of thesis

This thesis consists of five chapters. The first chapter introduces the previous literatures and content of the thesis. In second chapter, the procedure of the numerical scheme is described. Chapter 3 includes the information of target bridge description, traffic flow, and bridge monitoring, FE modelling and the validation of numerical scheme. Chapter 4 shows the application of the proposed numerical scheme in the target existing bridges with real traffic flow and local roughness damage. Chapter 5 concludes all the findings and contributions of the thesis with future research plan.

In the manuscript, Tables and Figures are included and all the citation references are listed at the end of thesis. The nomenclatures are presented in the beginning of the thesis and are consistent along the whole content. The detailed organization of the thesis is presented as follow:

Chapter 1 presents literature review, the motivation, aims and scope of the research. The outline of the thesis is then introduced in the end of the chapter.

Chapter 2 introduces the general description of numerical scheme and how it will be applied with given dynamic traffic data, bridge response and surface roughness condition.

Chapter 3 validates the proposed numerical scheme on a target existing bridge. It also describes the target bridge parameters, dynamic response and traffic monitoring on the bridge. A validated FE model of the test best structure is constructed. Parametric study on effects of traffic volume, speeds, vehicle passing order on bridge dynamic responses are investigated.

Chapter 4 applies the numerical calculated scheme to evaluate bridge dynamic responses and vehicle dynamic load effect on existing bridges considering traffic flow and local surface damage.

Chapter 5 concludes all findings and results of the thesis and proposes the future research study.

In this thesis, firstly, the general idea of combining effect of traffic flow and roughness condition in numerical scheme is constructed. Data acquisition and traffic monitoring are conducted in an existing steel box-girder bridge to extract the influenced traffic patterns on bridge oscillation. The measured acceleration is also used for validating the FE model of target bridge. The fluctuation of total load of car and truck considering the uncertainty of vehicle suspension parameters, speeds, and surface roughness condition are calculated. From extracted traffic patterns and statistical value of total vehicular load, traffic flow with random passing order of vehicles is constructed as transient time history loading function assigned on the deck node of the target bridge FE model. The simulated RMS of acceleration during 1- hour traffic which has high and small truck ratio are compared with measurement data for validating the numerical scheme. Using the validated scheme, effect of surface roughness condition and vehicle speed on bridge accelerations are statically investigated. Using the same numerical scheme, the effect of local roughness damage on dynamic effect of existing bridges is investigated. The surface roughness level is measured in term of international roughness index (IRI) at every 1-meter spacing on bridge deck. The value of IRI is then converted to the equivalent PSD of ISO road class. The assigned force of vehicle at Finite Element (FE) bridge node at 1-meter segment is generated from quarter car model simulation. Time history analysis is then implemented to evaluate the influence of traffic and local surface damage on dynamic responses and IM in existing bridges.

Chapter 2

2. GENERAL DESCRIPTION OF CALCULATION SCHEME

This chapter introduces the flow of proposed calculation scheme applied to estimate vehicle dynamic load effect on existing bridges considering traffic data and surface roughness. The proposed method will be applied for the next chapter to evaluate the vehicle dynamic load effect on existing bridge in case of random roughness condition and local roughness damage. The steps to simulate traffic flow from traffic volume data with different vehicle types, speeds, and random passing orders are described in detail. Firstly, traffic data and bridge acceleration are measured on the target structure. A validated FE model of the bridge is required for time history analysis. From the given traffic data, the generated input traffic load considering the effect of roughness condition is constructed. Finally, time history analysis is implemented in the available FE analysed software to evaluate bridge dynamic responses.

2.1 Flow of numerical scheme

2.1.1 General idea of numerical scheme

The scheme to statistically evaluate the vehicle load dynamic effect on existing bridges considering surface roughness and traffic flow is presented. The traffic data, the bridge response, the roughness profile, and the FE model of the target structure are required as the input for implementing the numerical scheme. Firstly, the acquired data are the bridge acceleration and the numbers each vehicle type passing through bridge at certain time interval. The length of time interval is considered in the traffic analysis; e.g., 5 minutes, 10 minutes. The extracted frequencies from measured acceleration are compared with simulated model shapes for validating the built-in FE model. Then, the traffic flow model with random passing orders of each vehicle type is constructed from the monitored traffic volume and assumed speed of traffic vehicles. At the same time, surface profile of the bridge deck should be measured on sites or generated from the available mathematical method. To consider the amplified effect of roughness irregularity on dynamic vehicular load, the surface profile is input into a vehicle roughness interaction simulation. The total load of vehicle in the simulation is calculated as the sum of static weight and the stochastic dynamic load amplified by roughness.

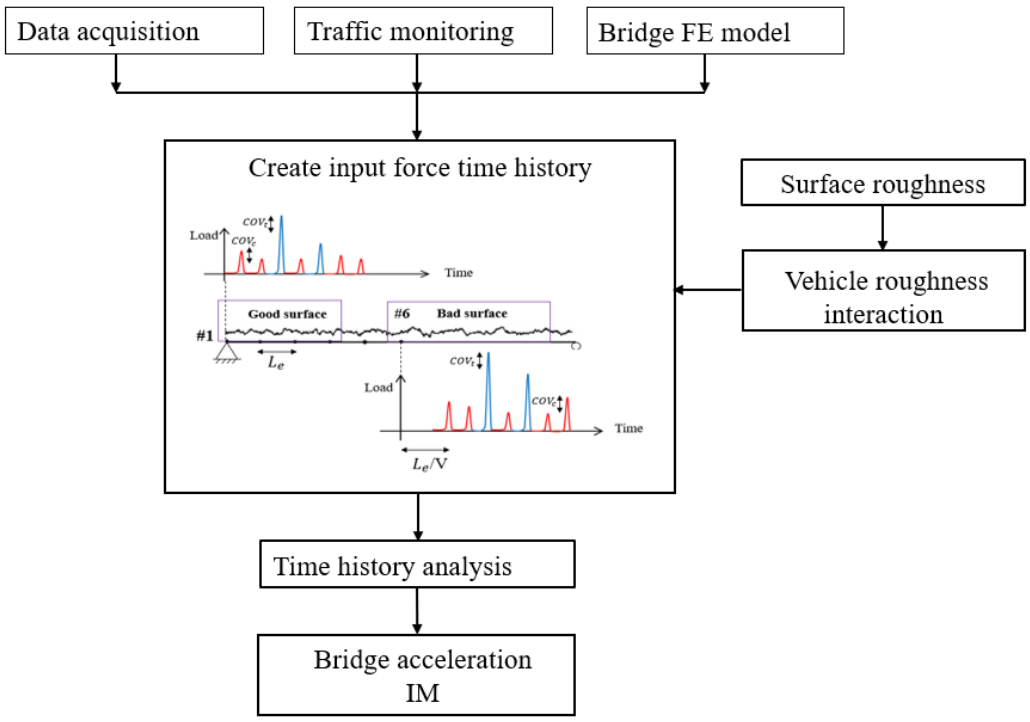

Figure 2.1: The flow chart of the numerical scheme

The fluctuation of total load of vehicle represents for the variation of vehicular load when traffic vehicles travel on given surface roughness profile. In proposed numerical scheme, each axle of vehicle is represented as an input force function. The amplitude of the forcing function is generated from statistical value of total load in vehicle surface roughness interaction. Meanwhile, the function shape is modelled as the positive part of cosine function with the period equal to four times of the traveling time of the time lag between two deck nodes in bridge FE model. The input force time history of traffic flow passing through each node on bridge deck is constructed from the chain of input force function of each vehicle type with random passing orders. The built-in input force is then assigned at each discretized node of bridge FE model. Time history analysis is implemented in Midas Civil to evaluate the bridge dynamic response and impact factor of traffic vehicles. The vehicle dynamic load effect on existing bridges considering combination effect of both random traffic and roughness condition could be investigated by the proposed numerical scheme. Fig. 2.1 presents the flow chart of implementing steps in numerical scheme.

2.1.2 Built-in traffic flow and bridge FE model

In this scheme, firstly, the random traffic flow is constructed from the measured traffic volume data of each vehicle type in a time interval. Traffic volume is defined as the number of vehicles passing through a section during a specific time interval. Assume that the traffic flow has is the averaged velocity V within the target time interval, that is derived using the relationship below:

$$N_{tr} = K \times V \tag{2.1}$$

where N_{tr}, K and V are traffic volume, traffic density and speed of traffic flow respectively. Traffic density is the number of vehicles per unit section. At the same traffic volume condition, the higher speed will reduce the density of traffic and vice versa. From given monitored traffic data, traffic flow with random passing orders is constructed. Consider a bridge structure with surface roughness under a traffic flow loading as shown in Fig. 2.2. Some assumptions were assigned to consider the traffic volume of each vehicles type acquired in the traffic data. In Fig. 2.2, two axial static loads of each vehicle, indicated by p_c and p_t are equal, and the time-lag between two axles of each vehicle, t_c and t_t are approximately calculated based on the distance of two axle spacing and vehicle speed V. The spacing distance between two axles of car and

truck were assumed to be 4 m and 8 m, respectively, which based on [61] for standard car and truck under 25 tons. Then, the characteristics of traffic flow within the setup time interval are applied for terming the time-history. The averaged heading time between consecutive vehicles $\overline{\Delta t}$ is calculated from the measured total traffic volume per the setup period. Also, the order of passing trucks is randomly sampled; for instance, in case of the traffic flow with total traffic volume of 100 and truck ratio of 10%, the ten numbers are sampled from #1 to #100. From the given assumptions, the random flow of measured traffic data is constructed.

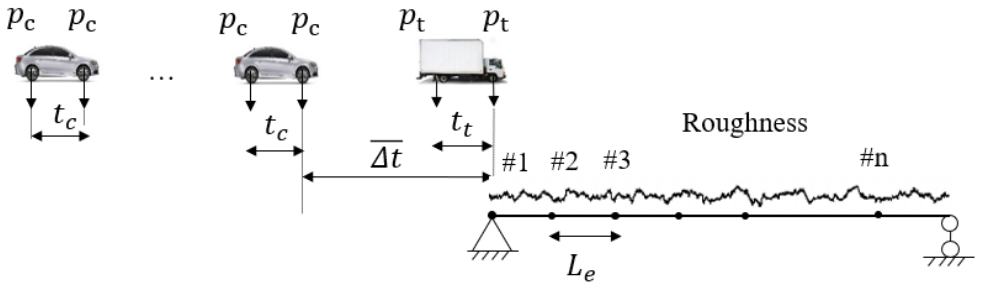

Figure 2.2 : Traffic flow pass through a bridge

At the same time, the FE model of the bridge is built from the designed document. The FE model is validated by comparing the calculated frequencies with the extracted frequency from measurement data. The deck of bridge FE model consists of nodes #1, #2, …, #*n* by the discretization. The built-in bridge FE model will be used for implementing time history analysis in the next step of the scheme.

2.1.3 Vehicle roughness interaction simulation

To investigate the variation of dynamic load due to surface roughness, the equations of motion between vehicle and roughness is constructed in vehicle roughness interaction simulation. In practice, the mass of vehicle is changed due to the additional load meanwhile the tire and suspension system performance may vary with their production series and service time even with the same vehicle type. In this study, traffic vehicles are classified as car and truck only. They are represented by quarter car model with uncertain parameters of vehicle mass, tyre and suspension system. In quarter car model simulation, effect of vehicle properties uncertainty, random properties of each roughness level, and the vehicle speeds on dynamic vehicle load are

investigated. If there is no available data for roughness measurement, the artificial random roughness is generated from available PSD value of each roughness level in International Standard Organization (ISO 8608). By solving the equation of motion between the quarter car model and simulated road profile, total load of car and truck the variation of vehicle parameter, roughness damage condition, and speeds are calculated. The total load is the sum of the amplified dynamic load due to random roughness and the static weight of vehicle. Consider that the calculated total load of traffic vehicle amplified by surface roughness is random at every point of bridge deck. The statistical values of the simulated total load (mean and COV) represent for the fluctuation of traffic vehicle load under different speeds and roughness conditions. Monter Carlo simulation with 10000 samples of each independence variable of vehicle parameters and roughness profile at each roughness level is generated by normal distribution. For each sample, mean and COV value of total load of car and truck is calculated. In the distribution of 10000 sample, we can randomly select sample #*k* of calculated mean of car and truck (P_{ck} and P_{tk}) and the respect COV (COV_{ck} , COV_{tk}) .The calculated random amplitude ($\tilde{P}_{cijk}$, $\tilde{P}_{tijk}$) of varying loads in front and rear tire of car #*i* and truck #*i* in the traffic flow at deck node #*j* on FE model from mean and COV sample #*k* are calculated as Eqs. 2.1 and 2.2. The considered steps of calculating varying load of traffic vehicle are presented in Fig. 2.3.

$$\tilde{P}_{cijk} = P_{ck}\left(1 \pm COV_{ck}\right) \tag{2.1}$$

$$\tilde{P}_{tijk} = P_{tk}\left(1 \pm COV_{tk}\right) \tag{2.2}$$

Where:

P_{ck} , P_{tk} : mean value COV value of total load of car and truck at sample #*k*

COV_{ck} , COV_{tk} : COV value of total load of car and truck at sample #*k*

$\tilde{P}_{cijk}$, $\tilde{P}_{tijk}$: random amplitude of constructed input load of car #*i* and truck #*i* at deck node #*j* at sample #*k*

This random amplitude of forcing function of each vehicle type represents for the variation of traffic vehicle passing though the surface profile on bridge. Moreover, each traffic volume data, the arrival of passing vehicles is randomly generated. The amplitude of varying

load will change for each single passing vehicle at each roughness point of bridge deck. From these values input force time history of traffic load will be constructed in the next step.

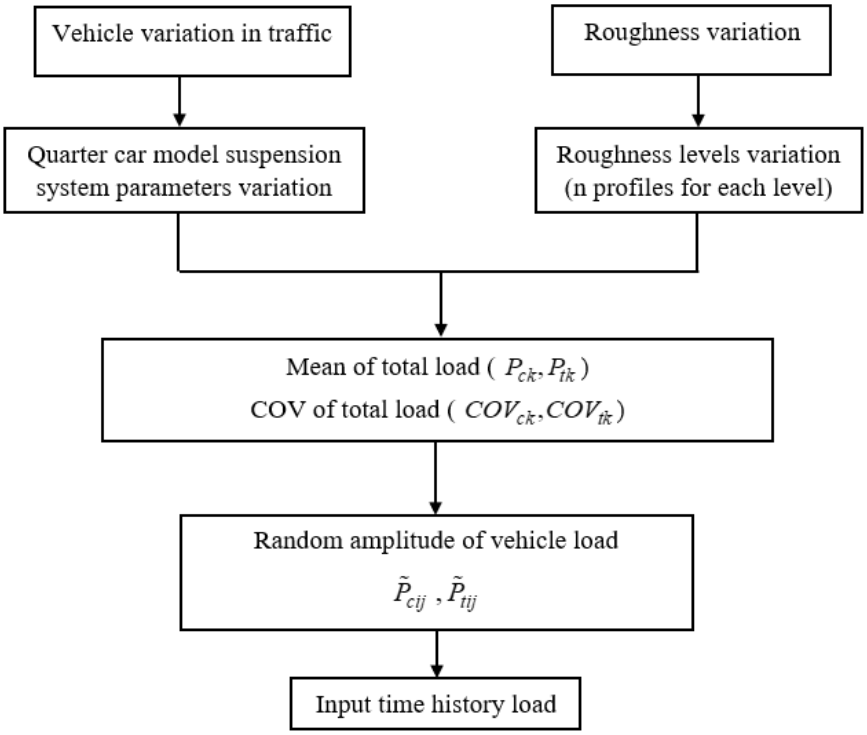

Figure 2.3 : Steps of construction of input traffic load

2.1.4 Input time history of traffic load

The main point of this scheme is that the dynamic effects of axial loads of passing vehicles are represented as a time-history of input force at each node of bridge FE model. From the random traffic flow and the statistical values of two total vehicle load, we could construct the input time history of traffic flow. Each axial load of a vehicle is assigned to the nodes of bridge deck model as two transient time forcing functions; i.e., two transient effects due to two axles for one vehicle. A dynamic vehicular load experiment was conducted to investigate the change of vehicle force amplitude and shape due to roughness condition. In the test setup, the impact wheel force of car and truck pass though the normal surface and a hump with different speed are measured by a load sensor. According to the experiment, the amplitude and shape of force change with speed and roughness level. The impact force can be modelled by a triangular

of cosine function. Therefore, in this study, the transient force function was represented by positive part of cosine functions with the amplitudes equal to the random total axle load. Detail of the experiment is provided in Appendix. The passing of a vehicle in built in random traffic flow is represented by the time-lag of the force function between two nodes t_e that can be determined by element size, L_e in Fig. 2.4, and the vehicle speed in the traffic flow V. The amplitude of force function of each of a passenger car and truck are random variables generated from normal distribution of mean and COV of calculated total load. To make sure that the load function increases from zero to load amplitude exactly at the bridge node, the period of cosine function must equal to four times of t_e.

Finally, the time history analysis is implemented for bridge dynamic response simulation in Midas civil. Fig. 2.4 shows the time history analysis time forcing function of truck and car assigned at node #1 and #2 of bridge deck. The dynamic effect of surface roughness, traffic flow, and speeds are investigated by maximum and RMS value of deck acceleration. This scheme provides a conventional tool for statistically assessing the combined effect of traffic flow and deck roughness condition on bridge dynamic response.

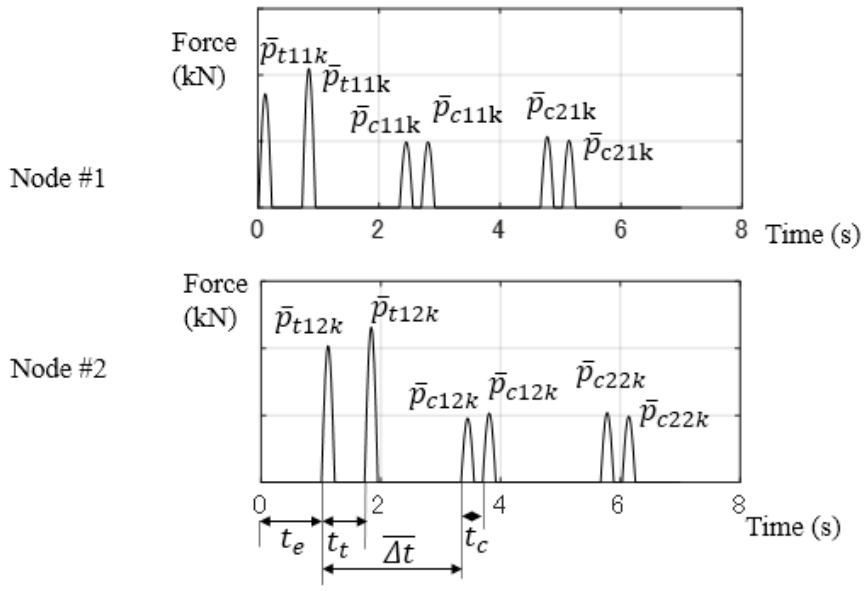

Figure 2.4 : Time history of input force function of truck #1, car #1 and car #2 at node #1 and #2 of bridge deck from sample #*k* of distribution of calculated mean and COV of total load

2.2 Summary

This chapter introduces the steps to implement the proposed numerical scheme on existing bridges considering the effect of traffic data and surface roughness. At first, number of each vehicle type passing through the target structures within a period is collected. From the traffic volume data and assumed vehicle speed, traffic flow model with random passing orders could be constructed. The headway time between consecutive vehicle in traffic flow is determined by traffic volume and the speed. At the same time of traffic monitoring, bridge acceleration is also measured on the target structure. Secondly, a FE model of the bridge constructed which define the discretized nodes on bridge deck. The calculated mode shape in FE model is compared with the frequencies extracted from the measurement for validation. Then, effect of roughness on dynamic load of each vehicle is calculated in vehicle roughness interaction. The vehicles are represented by quarter car model meanwhile the roughness must be measured or randomly generated by mathematical approach. The length of the roughness profile is equal to bridge length. The mean and COV of total load are calculated from quarter car model simulation. From the constructed traffic flow model and the statistical value of vehicle load, the input time history load of traffic flow passing through the discretized deck nodes is constructed. Each vehicle in traffic flow model is considered as a moving force function with fluctuated amplitude. The variation of forcing function amplitude is randomly generated from mean and COV of total load in vehicle roughness interaction simulation. Finally, the constructed input time history is assigned at each node of bridge FE model. Time history analysis is implemented in the available Midas Civil software to evaluate bridge dynamic responses and IM.

Chapter 3

3. VALIDATION OF NUMERICAL CALCULATION SCHEME

In this chapter, the parameters of target bridge, the dynamic data acquisition, and the traffic measurement are first presented. The correlation between the measured traffic and the bridge dynamic response were then verified using the acquired data for determining the significant traffic patterns for constructing the input traffic flow in the calculation. To evaluate the bridge dynamic response under traffic flow and roughness condition in numerical scheme, the quarter car model simulation was first implemented in this section. It calculates statistic variables; mean and COV, of the vehicle load at different speeds and random surface roughness levels. The statistical values are used for randomly generating fluctuated amplitude of the time history traffic forcing function. The dynamic response of the target bridge with the traffic flow forcing function created from the traffic data was then verified by comparing the calculated acceleration time-histories to the measured acceleration data. After the validation, the effect of the truck ratio, vehicle speed, and the surface roughness condition on bridge dynamic response are investigated by the parametric study.

3.1 Data acquisition in the target bridge and FE modelling

3.1.1 Target bridge description

The test-bed structure for validation here is one of spans of an existing steel box-girder bridge. The bridge is a half-through bridge, and the target span consists of three simply-supported steel box girders, a steel plate deck, and steel bearings. The target span has the length is 25.2m, and the widths of passenger lane and two vehicle lanes, which are in the same way, are 4m and 6.5m, respectively. Each of three box-girders is located at the edge of passenger or vehicle lanes (Fig. 3.1). Three main girders are connected by crossbeams every 2.52m in the longitudinal direction. The three girders are tapered along the longitudinal direction. The longitudinal ribs are placed every 0.3m in transverse direction to support the steel deck (Fig. 3.2). The slab of the girder has the thickness of 0.055 meter. Notice that no damages on the surface of asphalt concrete pavement is pointed out in the bridge inspection data; therefore, it can be said that the bridge surface is in good condition.

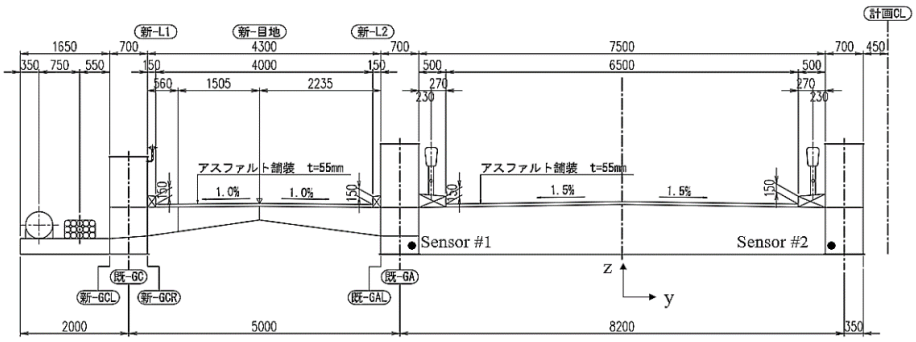

Figure 3.1: Cross section of the target bridge

(b) Cross beam and longitudinal rib system

Figure 3.2: The vehicle lane and cross beam of the target bridge

3.1.2 Acquisition of dynamic response data and traffic data

In the data acquisition, the synchronized accelerations were acquired by the wireless system [62], that mounted the MEMS sensor with measurement range of ±5G, 0.5μGrms/√Hz noise level, and 0.06μG/LSB resolution (product of Epson M-A351AU10). Two wireless sensor nodes; Sensor #1 and #2, were attached on the lower flanges at the mid-span of two box-girders of the traffic lanes, as shown in Figs. 3.3 and 3.4. The three-dimensional data were continuously acquired throughout the data acquisition period (from 8 am to 7 pm on January 11th, 2018) with 100Hz sampling frequency. The vertical acceleration (z direction) was used in this study.

The traffic volume data was also acquired on the bridge during the acceleration measurement. The number of cars and trucks pass through each of left and right lane of vehicle route of target structure were counted every ten minutes during data acquisition period. To characterize the variation of dynamic response with corresponding to traffic condition, the measured root mean square (RMS) of vertical acceleration were calculated. Fig. 3.5 shows the variation of traffic data and the RMS acceleration of bridge deck. From 8am to 7pm, total number of traffic and the number of cars show the same trend, meanwhile, the number of trucks decrease after 3pm (Fig. 3.5 (a)). From 8am to 3pm, the RMS of vertical acceleration in Sensor #2 (right lane) is always higher than Sensor #1 (left lane), however, the measured data in both sensors becomes the same at around 2 gal when the number of trucks reduce, as shown in Fig. 3.5(b). During that period, it is also observed that both number of trucks and RMS acceleration have decreasing trend.

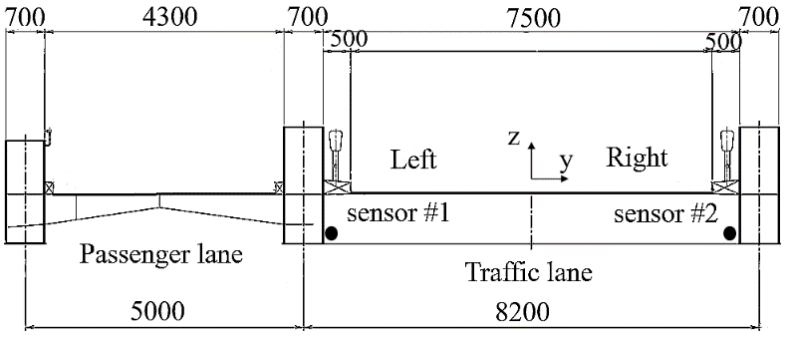

Figure 3.3: Target bridge span and configuration of wireless sensor nodes

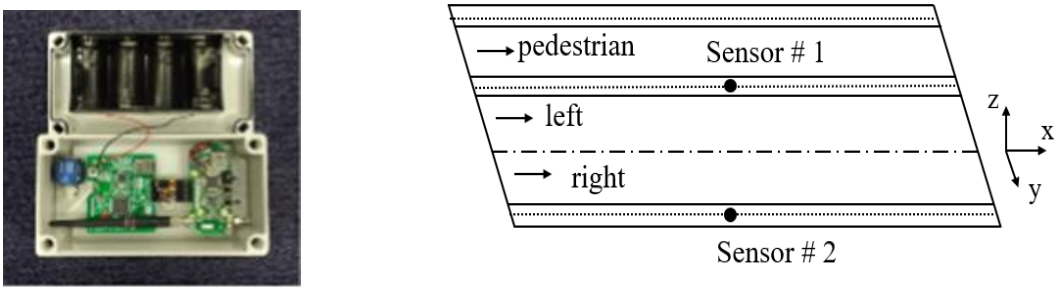

(a) Epson sensor (b) Sensor deployment

Figure 3.4: Target bridge span and configuration of wireless sensor nodes

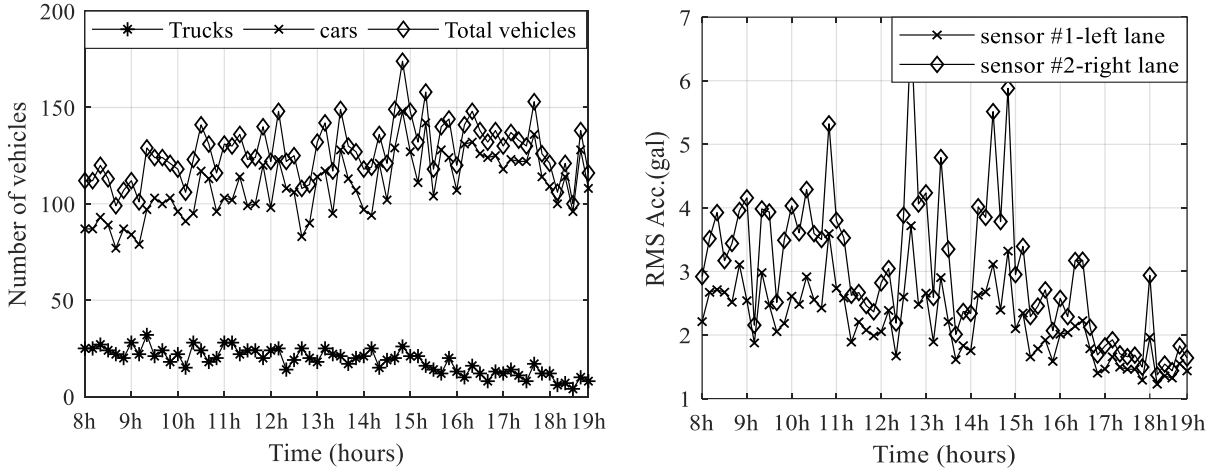

(a) Traffic volume (b) RMS of vertical acceleration

Figure 3.5: Traffic data and RMS of vertical acceleration of bridge from 8 am to 7 pm

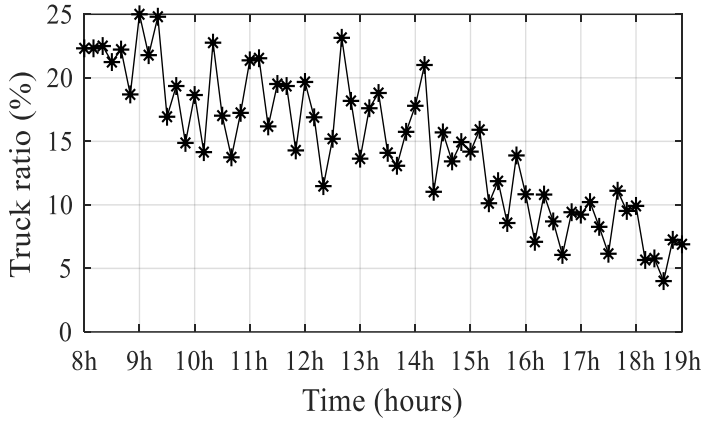

Figure 3.6: Truck ratio of traffic data from 8 am to 7 pm

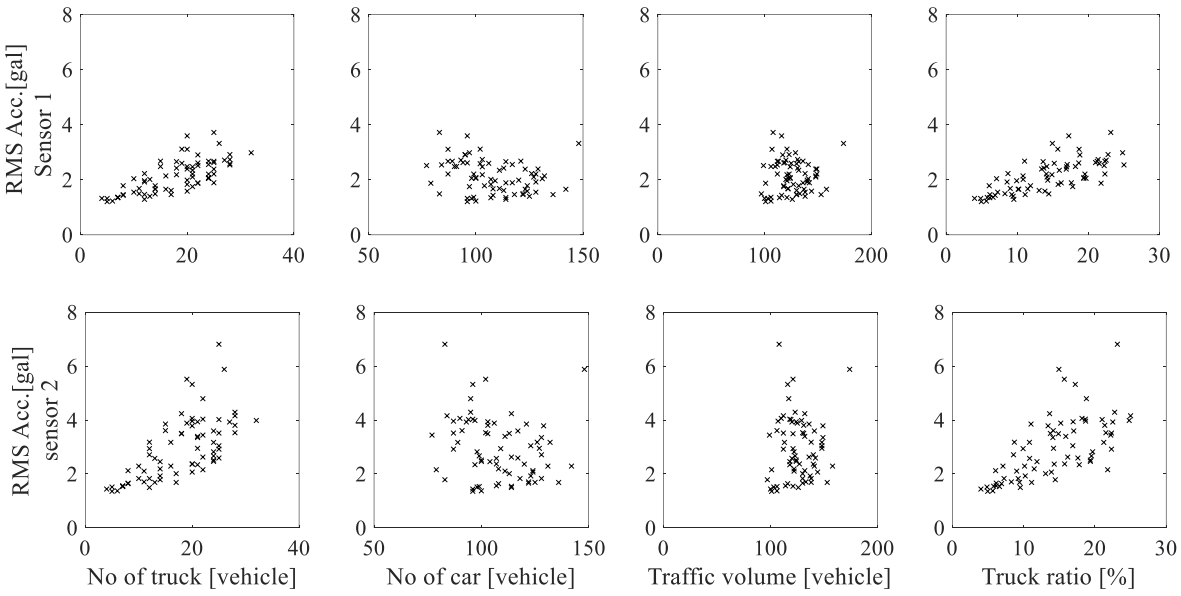

Figure 3.7: Scatter plots of traffic data with RMS of vertical acceleration from 8 am to 7 pm

From monitoring data, the number of trucks over the total vehicle numbers (truck ratio) is also calculated (Fig. 3.6). The relationship between bridge dynamic response and traffic data are presented in Fig. 3.7. Each point of the graph represents for the RMS of vertical acceleration measured by sensor 1 and 2 corresponding to the number of trucks, cars, traffic volume, and truck ratio of a 10-minute traffic data. The scatter plot indicates that there is positive correlation between the number of trucks and truck ratio with RMS acceleration. On the other hand, traffic volume has no influence on bridge dynamic response since the acceleration results variate at the same number of vehicles. It is also seen that the increase of car reduces the RMS acceleration. To quantify the relationship of traffic data with the bridge dynamic response, the correlation coefficients between measured RMS of vertical acceleration with number of counting vehicles and truck ratio were calculated, as shown in Table 3.1.

The results show that bridge dynamic response has high correlation with number of trucks and truck ratio meanwhile it has low correlation with number of cars. It indicates that the truck or heavy vehicle significantly contributes to the bridge oscillation; meanwhile, the RMS acceleration is independent of traffic volume. Therefore, the main traffic patterns that are considered in the numerical simulation is the speed and truck ratio. The relationship between RMS acceleration and truck ratio can be used for validating the results of the numerical scheme.

Table 3.1: Correlation coefficient between traffic data and RMS of vertical acceleration

Traffic data	Sensor 1	Sensor 2
Number of trucks	0.72	0.66
Number of passenger cars	-0.27	-0.21
Total passenger cars and trucks	-0.04	-0.07
Truck ratio	0.72	0.64

3.2 Construction of a FE model

3.2.1 FE modelling

To implement time history analysis, a finite element (FE) model of the target span was constructed by one of general-purpose software: Midas Civil (version 2015). The cross-section and detail length of structure components were modelled according to the bridge drawing in design stage. The main girders, crossbeams and longitudinal ribs were modelled as the beam elements; meanwhile, the deck slab was modelled by the plate element (Fig. 3.8). The simply-supported boundary conditions were applied in the both ends of three main girders in the target span. All the model components were designed with SM490A steel material with Young modulus of 2.05×10^8 MPa and Poisson ratio of 0.3 (Table 3.2). The total model consists of 1,096 beam elements and 680 plates elements. The target structure was an existing bridge; however, the FE model was built based on parameters provided in the design document. Assume that density of deck slab concrete was 24 kN/m^3 and the cross section of all cross-beam was the same across bridge width. The modal analysis was conducted for the constructed FE model, as shown in Fig. 3.9.

Table 3.2: Parameters of the target bridge

Parameters	Description	Values
Young's modulus of steel	γ_s	20.5 GPa
Young's modulus of concrete	γ_c	20 GPa
Steel's density	D_s	7.7 g/cm3
Concrete's density	D_c	2.4 g/cm3
Poisson ratio of concrete	ρ_c	0.17
Poisson ratio of steel	ρ_s	0.3

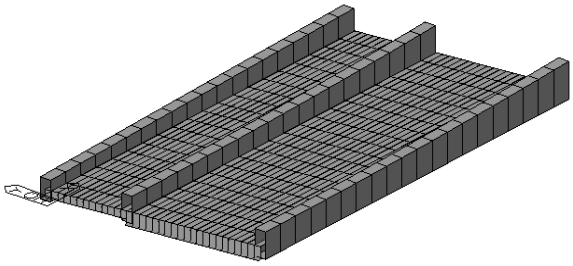

(a) FE bridge model

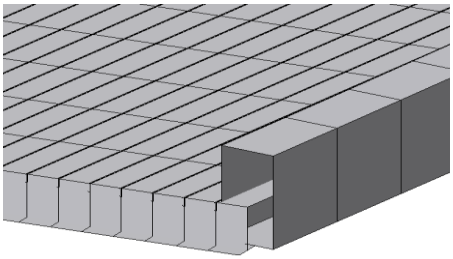

(b) Girder and slab

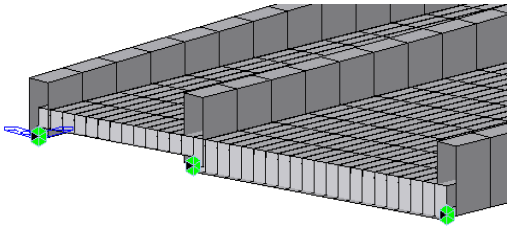

(c) Boundary condition

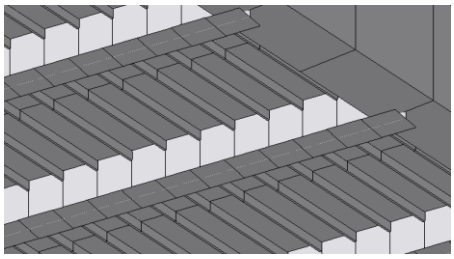

(d) Cross beam and longitudinal ribs

(e) The tapered girder

Figure 3.8: The components of constructed FE model

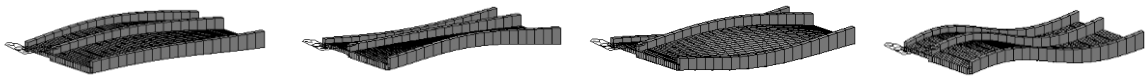

(a) 1st mode (b) 2nd mode (c) 3rd mode (d) 4th mode

Figure 3.9: Mode shapes in bridge FE model

3.2.2 FE modelling validation

To extract the measured resonant frequencies for FE model validation, the power spectrum density (PSD) of 10-minute acceleration was calculated. The peak frequencies were derived from one of acceleration data from 13:40 pm to 13:50 pm. Each time-history was

divided into four segments to apply the Hanning window and 50% overlap. From the obtained PSD in Fig. 3.10, four peaks can be recognized. The comparison of calculated and measured frequencies is shown in Table 3.3. The discrepancy in the 2nd mode is relatively high; however, there are good agreement around 95% in three of four modes. The FE model of target structure is validated for implementing time history analysis.

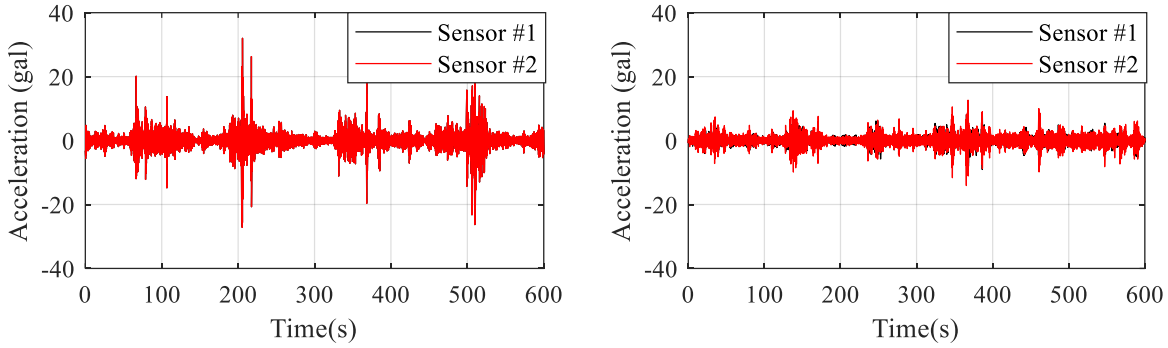

(a) High truck ratio (8 am to 8:10 am) (b) Low truck ratio (6:10 pm to 6:20 pm)

Figure 3.10: Time history of measured vertical deck acceleration at high and low truck ratio

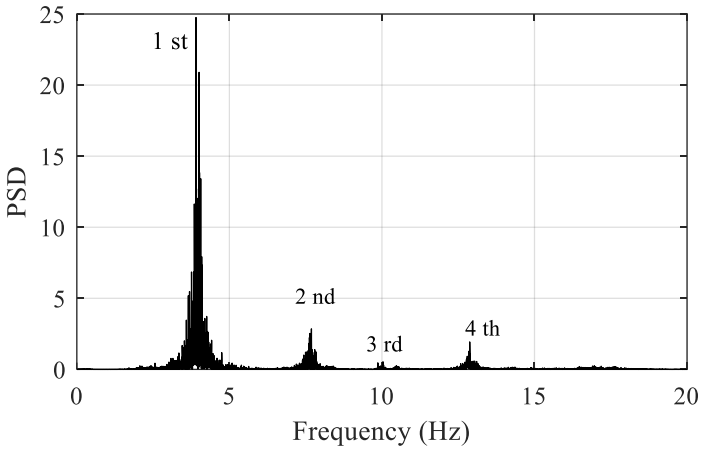

Figure 3.11: PSD of measured frequencies of target structure

Table 3.3: Comparison of resonant frequencies of FE model to measurement data

Mode no.	FE model (Hz)	Measurement (Hz)
1st	4.17	4.02
2nd	6.21	7.76
3rd	10.79	10.06
4th	13.36	12.89

3.3 Statistical variables of vehicle load

3.3.1 Road profile generation from roughness index

Previous literatures [13], [15], [16] found that the variation of vehicle loads is significantly influenced by the condition of roughness surface. When a vehicle moves on the bridge, the total load of the vehicle is different from its static weight as the dynamic load amplified by irregularity surface and vehicle velocity. The aim of this section is to quantify the variation of total load of car and truck under certain roughness levels and different speeds. The mean and COV values of output load represent for the interaction between vehicles and different random surface condition. From the statistical results, the amplitude of time forcing function of each vehicle in traffic flow amplified by surface roughness will be randomly generated by normal distribution for time history analysis.

The most common way to create an artificial roughness is based on the PSD value of road profile indicated in ISO 8608 [43]. The ISO road provides the PSD $g_d(n_0)$ (m^3/cycle) at the reference spatial frequency $n_0=1/2\pi$ (cycle/m) of the road level from very good to very bad condition. From this value, the PSD function $g_d(n)$ of road profiles at spatial frequency n (cycle/m) is calculated by Eq. (3.1)

$$g_d(n) = g_d(n_0)\left(\frac{n}{n_0}\right)^{-2} \quad (n_1 \le n \le n_2) \tag{3.1}$$

where n_1, n_2 are the lower and upper cut-off frequency of the road profile, respectively. The wave length of the current simulation is from 0.02 m to 25 m. The random road profile $h(x)$ is the sum of simple harmonic functions as expressed in Eq. (3.2)

$$h(x) = \sum_{i=0}^{N} \sqrt{2\Delta n \cdot g_d(i\Delta n)} \cos(2\pi i \Delta n \cdot x + \varphi_i) \tag{3.2}$$

In the equation, the random phase angle φ_i of harmonic functions can be generated from a uniform probabilistic distribution within 0 to upper band 2π and spatial wave number Δn (cycle/m). To assess effect of surface roughness levels, the random deck profile from good, average, and bad condition of bridge surface which correspond to PSD of 32×10^{-6}, 128×10^{-6} and 512×10^{-6} (m^3/cycle) are generated at every 0.05 m along the length of the target bridge (25.2 m). The artificial random roughness profiles are shown in Fig. 3.12. It is observed that

the profiles fluctuate within ±5 mm, ±10 mm, and ±20 mm at good, average, and bad surface roughness level. The plot of PSD of generated profiles is given in Fig.3.13.

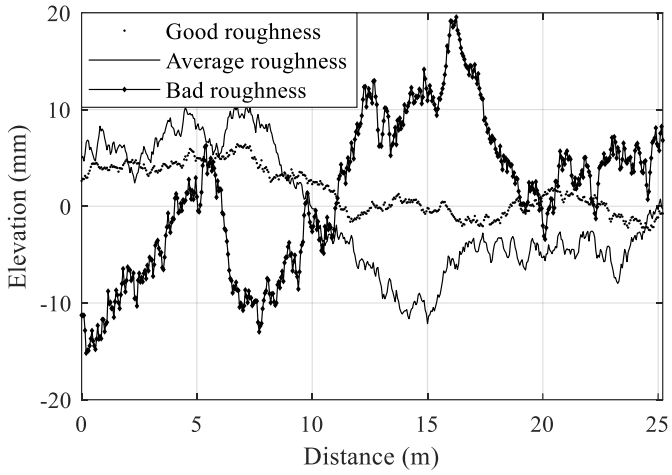

Figure 3.12: Generated random roughness in good, average, bad condition from ISO 8608

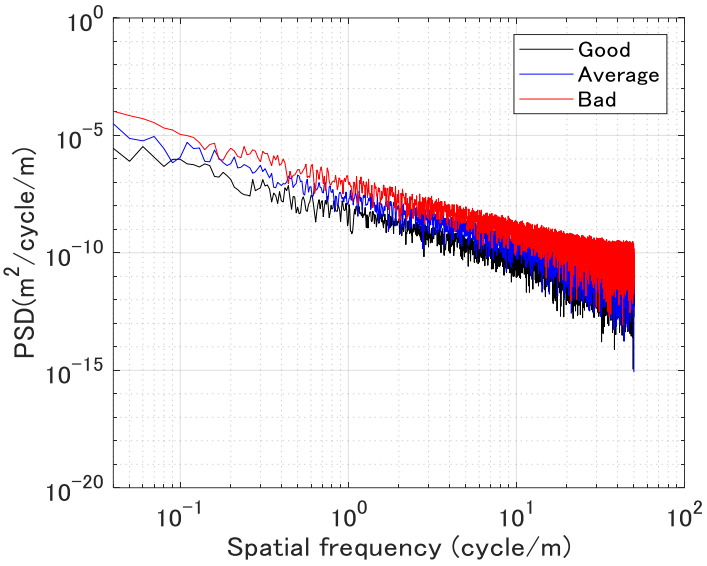

Figure 3.13: PSD of generate profiles

3.3.2 Quarter car model

The variation of vehicle load under different levels of roughness is investigated by the quarter car models. In this simulation, the traffic vehicles are classified as car and truck. The lumped-mass modelling and uncertainty parameters of the car and truck quarter car models are given in Fig. 3.14 and Table 3.4 [63-66]. Each parameter of vehicle suspension is generated randomly and independently as normal distribution with the given mean and COV value. The

interaction of quarter car model and random roughness is characterized by instantaneous displacement of sprung mass y_2, un-sprung mass y_1, and the height of roughness h with respect to the road distance x, as shown in Fig. 3.14.

Table 3.4: Parameters of quarter vehicle models [63-66]

Parameter	Mean-Car	Mean-Truck	COV Car	COV Truck
Sprung mass m_s (kg)	400	4,500	10%	20%
Un-sprung mass m_u (kg)	40	650	10%	20%
Suspension stiffness k_s (kN/m)	21	570	10%	20%
Suspension damping c_s (N·s/m)	1,500	21,000	10%	20%
Tire stiffness k_t (kN/m)	150	3,000	10%	20%

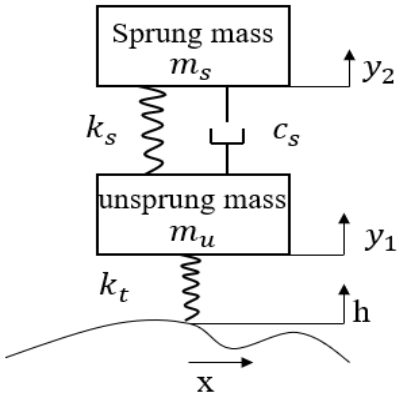

Figure 3.14: Quarter Car Model

When vehicle passes through the road profile, the equations of motion between quarter car model and random road roughness are given in Eqs. (3.3a) and (3.3b)

$$m_s\ddot{y}_2 + c_s\left(\dot{y}_2 - \dot{y}_1\right) + k_s\left(y_2 - y_1\right) = 0 \tag{3.3a}$$

$$m_u\ddot{y}_1 + c_s\left(\dot{y}_1 - \dot{y}_2\right) + k_s\left(y_1 - y_2\right) - k_t\left(y_1 - h\right) = 0 \tag{3.3b}$$

The fluctuation of dynamic load when vehicles travel on the certain random road profile is calculated via the stiffness of un-sprung mass k_t and relative displacement between road profile and un-sprung mass, as expressed in Eq. (3.4). The total load of vehicle P_{total} is the sum of the dynamic load P_{dyn} with the dead load $(m_u+m_s)g$ of vehicle as shown in Eq.(3.5).

$$P_{dyn} = k_t \left(h - y_1 \right) \tag{3.4}$$

$$P_{total} = P_{dyn} + \left(m_u + m_s \right) g \tag{3.5}$$

where g=9.81m/s^2 is the gravity acceleration of vehicle weight. In this study, 10 random roughness profiles are generated to reduce the bias of the simulation on dynamic load. The investigated speeds of quarter car models in the simulation are 20, 40, 60, 80 km/h, respectively.

3.3.3 Dynamic axle load under different surface roughness level and speeds

At each road profile case, the mean and COV of total load of car and truck travel on the bridge at a certain speed are calculated. Figs. 3.15 plots the instantaneous dynamic force of car and truck at different speeds in good surface condition. The figure indicated that as the vehicle speed increases, the dynamic load of car does not change but the travel time on the bridge reduces. As a result, the calculated mean total load and the calculated COV is the same when the speeds of vehicles increase as shown in Figs. 3.18(a) and 3.19 (a). Figs. 3.16 and 3.17 plot the instantaneous total force of car and truck at different surface condition at speed of v=20 km/h. The load of vehicle is more fluctuate when the roughness condition deteriorated.

Figs. 3.18 and 3.19 present the error plots of standard deviation of each of mean and COV of the total loads of car and truck under the different roughness conditions in 20 running cases. It is observed that both values are more fluctuated at deteriorated roughness condition. In both cases of truck and car, the COV of total load increases roughness condition deteriorated as shown in Fig.3.18. It is observed that both values are more fluctuated at deteriorated roughness condition, however, they keep the same value at different speeds. In both cases of truck and car, the COV of total load significantly increases as roughness condition is more damage, as shown in Fig. 3.19. Comparing two vehicle types, truck is much more influenced by roughness condition as its COV is always higher than car at all speed levels. It needs to be pointed out that the statistical values of total load could represent for the interaction between traffic vehicle and different surface roughness condition. The statistical values from all 20 cases of random surface profile are averaged to extract the calculated mean and COV of total load in quarter car model simulation. The values are then used for generating the random load fluctuation of car and truck in traffic flow due to different roughness conditions for time history analysis (as shown in Eqs. 1.1 and 1.2).

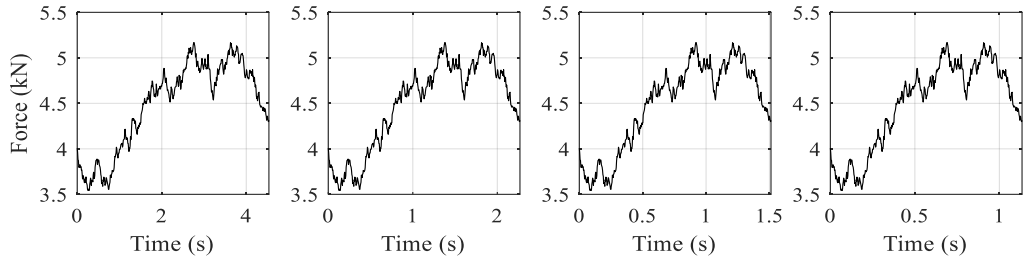

(a) V= 20 km/h (b) V= 40 km/h (c) V= 60 km/h (d) V= 80 km/h

Figure 3.15: Dynamic load of car travels on good surface roughness at different speeds

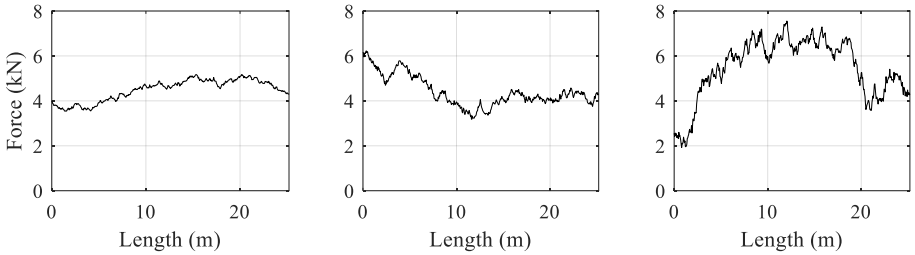

(a) Good roughness (b) Average roughness (c) Bad roughness

Figure 3.16: Dynamic load of car travels on different surface roughness at v=20 km/h

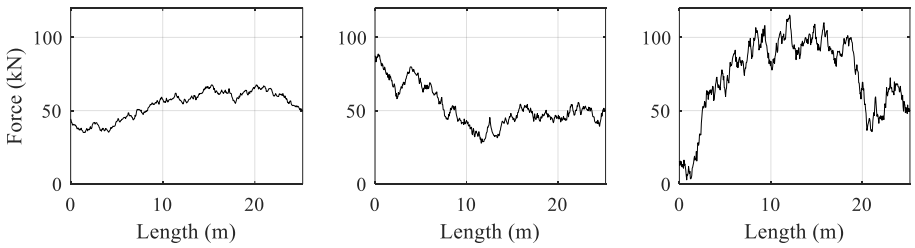

(a) Good roughness (b) Average roughness (c) Bad roughness

Figure 3.17: Dynamic load of truck travels on on different surface roughness at v=20 km/h

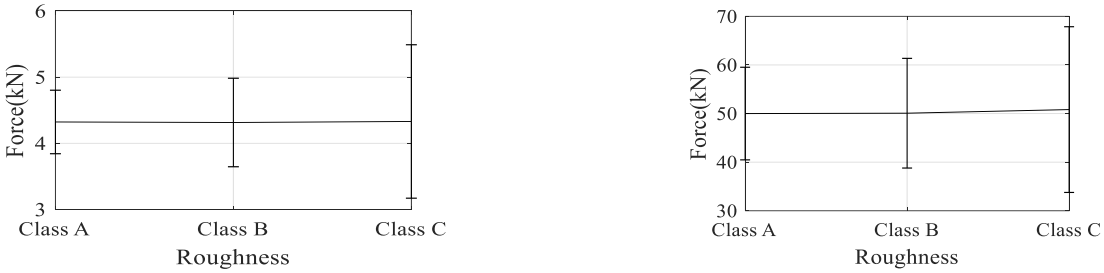

(a) Mean of total load of car (b) Mean of total load of truck

Figure 3.18: Error bar plot of mean of total load of car and truck under different roughness conditions

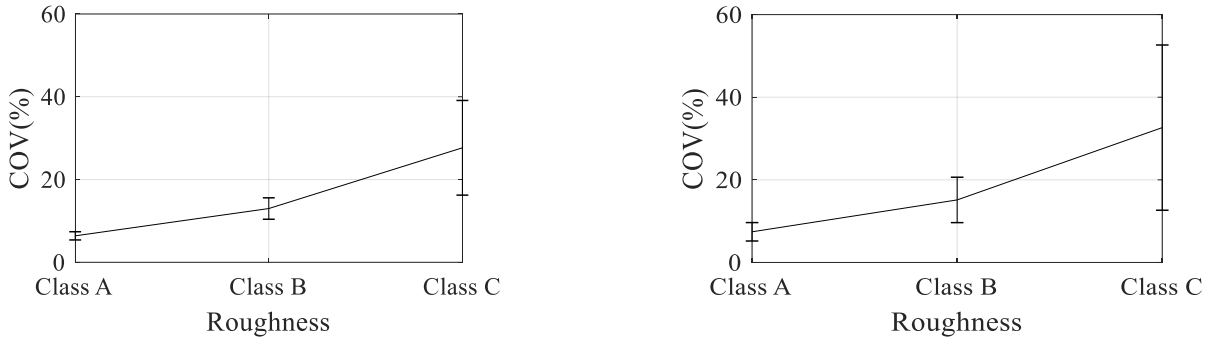

(a) COV of total load of car (b) COV of total load of truck

Figure 3.19: Error bar plot of COV of total load of car and truck under different roughness conditions

3.4 Validation of numerical calculated scheme

To evaluate the bridge dynamic response under traffic flow and roughness condition in numerical scheme, the quarter car model simulation was first implemented in this section. It calculates statistic variables; mean and COV, of the vehicle load at different speeds and random surface roughness levels. The statistical values are used for randomly generating fluctuated amplitude of the time history traffic forcing function. The dynamic response of the target bridge with the traffic flow forcing function created from the traffic data was then verified by comparing the calculated acceleration time-histories to the measured acceleration data. After the validation, the effect of the truck ratio, vehicle speed, and the surface roughness condition on bridge dynamic response are investigated by the parametric study

In section 3.2, it is found that the RMS of measured acceleration has positive correlation with truck ratio of traffic flow. Therefore, RMS accelerations under different truck ratio are compared with data acquisition results for time history analysis validation. Bridge dynamic response is calculated during 1- hour length traffic data with high and low traffic ratio. The high truck ratio traffic is from 8 am to 9 am at which the number of trucks accounted for approximate 20% of total vehicles. Meanwhile, truck ratio is lower than 10% from 6 pm to 7 pm. For each traffic condition, ten loading scenarios are implemented to roughly express the random feature of traffic flow. The simulation was implemented by constant Newmark-beta integration method in Midas Civil software with 0.01-second time increment and 5% damping ratio. According to monitoring data, traffic flow runs in two lanes of the bridge at the same direction. Since the deck surface of test-bed structure is in good condition, the time forcing function of traffic

vehicles is built from the calculated mean and COV of total load under good roughness surface. Assume that the traffic has the constants speed of 20 km/h in time history analysis. Time history of calculated acceleration during 10-minute traffic flow at high truck ratio (8 am to 8:10 am) and low truck ratio (6 pm to 6:10 pm) are shown in Fig. 3.20. It is observed that the visible peaks of simulated acceleration represent for the number of trucks in traffic flow. Since the traffic vehicles travel on two lanes, the acceleration amplitude increases when vehicles run parallel on the bridge. As a result, truck ratio in traffic flow influences on RMS value of acceleration rather than its maximum. To investigate the sensitivity of bridge dynamic responses and the number of passing order, the standard error bar plot of RMS calculated acceleration value with 5, 10, 15 and 20 passing orders of the same traffic condition are implemented in Fig. 3.21. The results show that the number of passing order should be larger than 10 to get the stable result of bridge dynamic responses. Figs. 3.22 and 3.23 compare the measured and error bar plot of calculated RMS accelerations at right and left side of mid-span deck during 1-hour traffic at different truck ratios.

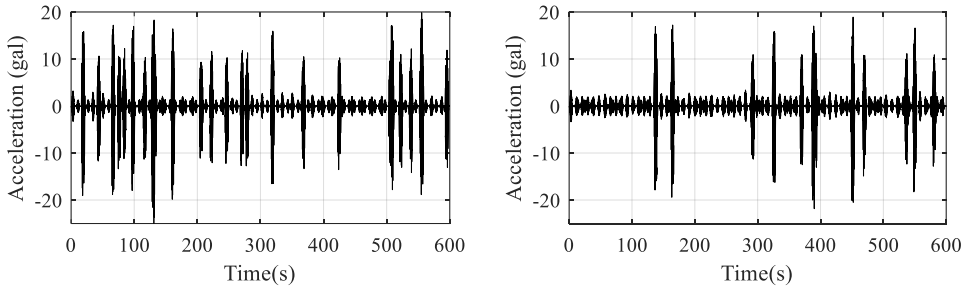

(a) High truck ratio (8 am to 8:10 am) (b) Low truck ratio (6 pm to 6:10 pm)

Figure 3.20: Time history of calculated acceleration during 10-minute traffic flow

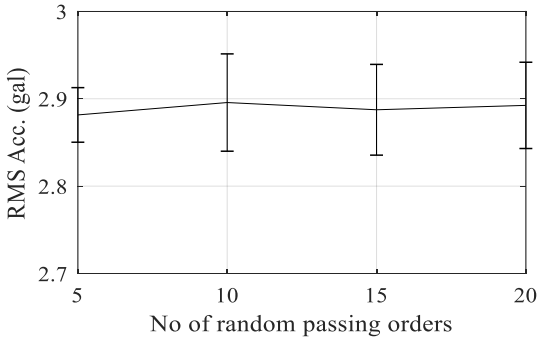

Figure 3.21: Error bar plot of RMS Acceleration with number of random passing orders

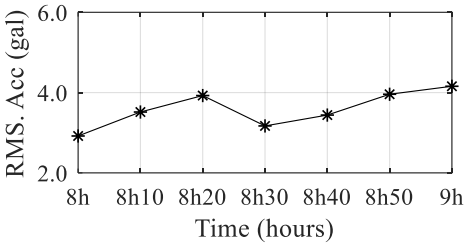

(a) Measured acceleration at right lane

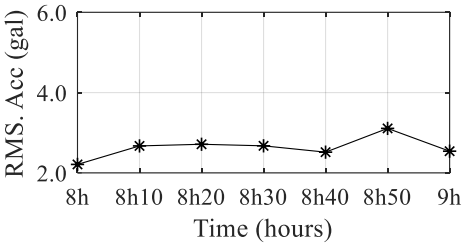

(b) Measured acceleration at left lane

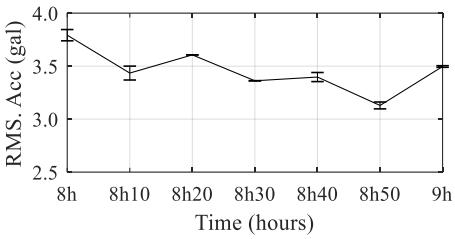

(c) Error bar plot of acceleration at right lane

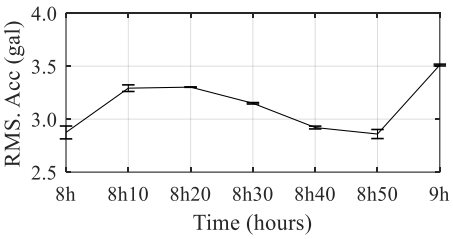

(d) Error bar plot of acceleration at left lane

Figure 3.22: RMS of measured and calculated acceleration at high truck ratio condition

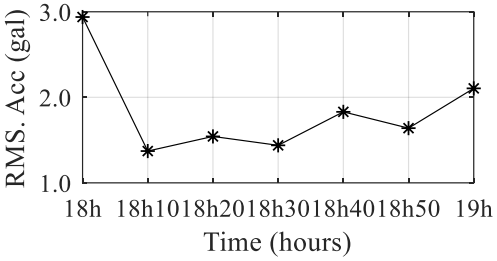

(a) Measured acceleration at right lane

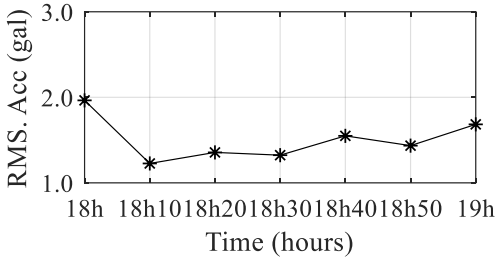

(b) Measured acceleration at left lane

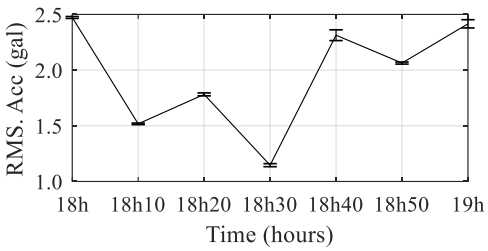

(c) Error bar plot of acceleration at right lane

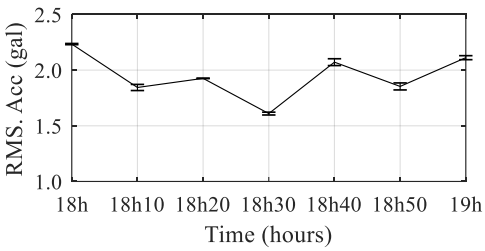

(d) Error bar plot of acceleration at left lane

Figure 3.23: RMS of measured and calculated acceleration at low truck ratio condition

Since the weight and speeds of vehicle are neither identified in real case, only fluctuation trend of RMS acceleration under different traffic condition are compared with monitoring data. When traffic flow has high truck ratio (8 am to 9 am), the calculated response could capture the shift of RMS acceleration in the measurement acceleration except for some sets of data period (i.e. from 8 am to 8:10, 8:40 to 8:50 am of Figs. 3.22 (a), 3.22(c)). On the other hand, in the case of low truck ratio (6 pm to 7 pm), the RMS fluctuation of calculated acceleration agreed with that of measurement data. It is observed that the high fluctuation of truck weight on traffic flow affected on the RMS of bridge accelerations. In addition, higher calculated RMS accelerations are also observed at high truck ratio condition (8 am to 9 am) as compared with low truck ratio condition (6 pm to 7 pm). It could be concluded that RMS acceleration depends on truck ratio of traffic flow. Since this finding has good agreement with measurement data, the proposed numerical scheme could capture fluctuation of bridge dynamic response under different traffic condition and good surface roughness.

3.5 Effect of traffic flow characteristics and roughness conditions

3.5.1 Bridge acceleration

It has been reported that the deterioration of surface roughness and vehicle speed have significant effect on bridge responses. Time history analysis is further applied for bridge dynamic evaluation to assess the influence of these factors. RMS and maximum values of acceleration which represent for the average and instantaneous fluctuation level of bridge dynamic responses are calculated. Traffic flow at 8am to 8:10 am with volume of 112 vehicles and 22.3 % truck ratio are chosen for parametric study. At different speeds and roughness conditions, ten loading scenarios of the given traffic condition are analysed. At each scenario, the passing orders of truck and car are randomly generated.

Figs.3.24 and 3.25 plot the standard error bars of RMS and maximum value of deck acceleration at mid span under good, average, bad surface roughness and vehicle speed of 20 to 80 km/h. The results show that RMS values of acceleration increase with the increment of vehicle speeds meanwhile they keep the same at all roughness conditions. The RMS values only slightly increase when traffic passes through bad roughness condition at 60 to 80 km/h speed (Fig. 3.23 (c)). On the other hand, the maximum value of bridge acceleration is influenced by both speeds and surface irregularity. The mean value of maximum acceleration is more

fluctuated when traffic vehicle travel on deteriorated surface condition, except for the case of low speed (20 km/h). It can be explained that the fluctuated load of car and truck under high speeds and damaged roughness could result in the high instantaneous bridge acceleration.

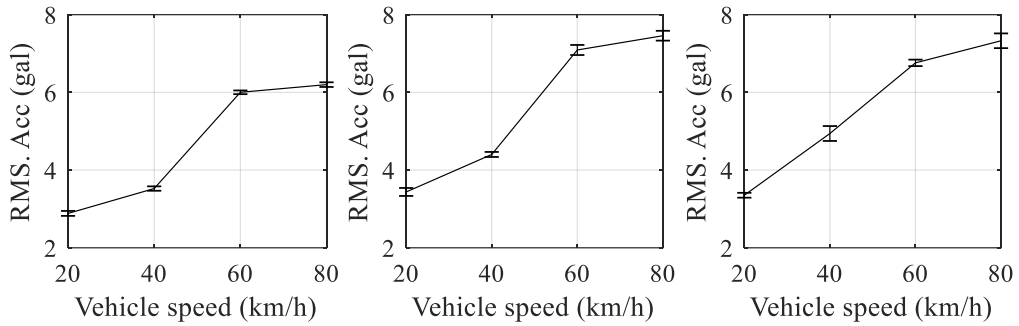

(a) Good roughness (b) Average roughness (c) Bad roughness

Figure 3.24: RMS acceleration under different surface roughness and speeds

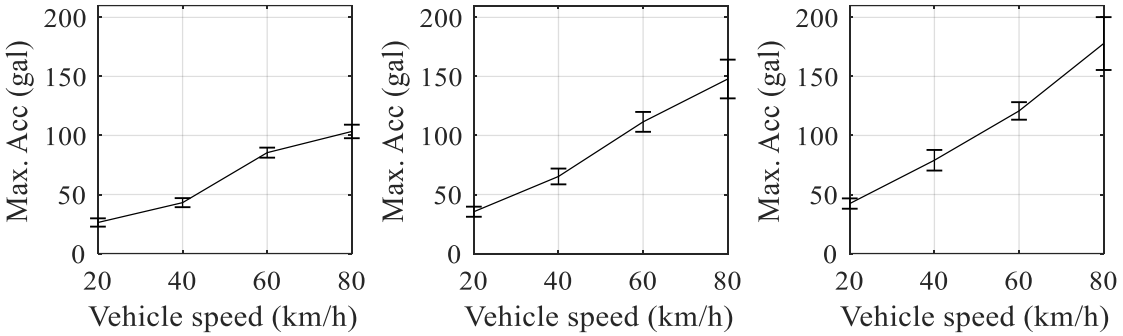

(a) Good roughness (b) Average roughness (c) Bad roughness

Figure 3.25: Maximum acceleration under different surface roughness and speeds

The numerical results indicate that RMS of deck acceleration depends on traffic condition and speed meanwhile its maximum value is amplified by deteriorated roughness surface and high vehicle velocity. From the results here, the features of RMS and maximum accelerations obtained by the calculation scheme are expected to be used for the evaluation of the bridge dynamic effects on live load in the existing bridges.

3.6 Summary

In this study, authors proposed a numerical calculation scheme to evaluate the bridge dynamic response under the traffic flow amplified by surface roughness condition for assessing dynamic effect of live load in the existing bridges. At first, the detail parameters of target bridge, data acquisition and traffic monitoring data on the bridge are presented. A validation FE model is also constructed for using in time history analysis. The correlation result shows that RMS acceleration and number of trucks or truck ratio has high correlation meanwhile it is independence of number of total vehicle and number of cars. The bridge dynamic data, traffic data, and FE model of the target bridge will be used for validating the numerical scheme in the next chapter.

The scheme illustrated the combined effect of traffic flow and surface roughness irregularity by fluctuated amplitude of loading function assigned at the bridge nodes of the FE model. From verifications with the target of an actual bridge and the numerical study, some conclusions can be summarized as below:

- From monitoring data, the number of trucks or truck ratio in traffic flow have high correlation with RMS of bridge acceleration. In numerical scheme, the calculated bridge accelerations during 1- hour traffic with high and low truck ratio also showed agreements with that of the measurement data, especially in case of low truck ratio.

- From the parametric study, the RMS acceleration increases with the increment of vehicle speed mean while it slightly changes from good to bad surface condition. At the same traffic condition and speed, the RMS acceleration did not fluctuate among different passing orders of traffic vehicles.

- The parametric study showed that the variation of vehicle speed, vehicle passing order, and surface roughness condition influences on maximum of bridge acceleration. The value is independence of truck ratio; however, it is influenced by both speed and surface roughness condition. The maximum acceleration is also highly fluctuated by variation of vehicle passing order in traffic flow, especially at high speed and bad surface roughness.

In the proposed calculation scheme, the different damage conditions of surface roughness along bridge length can be represented by statistically traffic load with different fluctuated level. Therefore, the constructed scheme is expected to evaluate the effect of local surface

deterioration of the actual surface roughness and traffic flow on dynamic responses. It was then concluded that the calculation scheme was applicable to evaluate dynamic responses of existing bridges with the given dynamic monitoring data, traffic flow, and surface roughness condition.

Chapter 4

4. VEHICLE DYNAMIC LOAD EFFECTS ON EXISTING BRIGES CONSIDERING LOCAL ROUGHNESS DAMAGE

When traffic flow continuously passes through the bridge, the peak of vehicle load often occurs at the specific damaged locations of bridge surface. As a result, the continuous spatial repeatability phenomenon increases the deteriorated level of surface roughness and fluctuates bridge dynamic responses. This chapter presents an investigation of vehicle dynamic load effect on existing multiple reinforced concrete bridges considering traffic flow and local roughness condition by using the proposed scheme. The local damage of bridge surface is measured by International Roughness Index (IRI) in every 1-meter length. The value of IRI is then converted into PSD of road roughness level in ISO 6808. The value of PSD represented for road roughness classification of each segment on bridge. The proposed numerical scheme is applied to calculate bridge dynamic response and IM of the bridges considering roughness condition indicated in

each segment length. To validate the scheme, RMS acceleration of bridge deck in different set of traffic oscillated by measured surface condition are compared to the measured acceleration. Effect of local damage condition and vehicle passing orders on the bridge dynamic responses is also examined. Dynamic effect ratio on bridges considering the traffic and local damage is derived, which relate to the dynamic impact factor in LRFR specification.

4.1 Data acquisition and traffic monitoring

This section presents the procedure of bridge measurement and traffic counting in two existing bridges in Vietnam. At first, the information of bridge parameters is provided. In data acquisition, the mid-span deck acceleration and traffic volume are measured every 5 minutes. Bridge acceleration is measured by two sensor nodes attached near to the railing in the middle and the quarter of the bridge length. Total of 7 sets of results will be used to statistically evaluate the mean and standard deviation of bridge dynamic responses, number of vehicles and percentage of truck pass through the bridge. The

4.1.1 Bridge parameter and sensor deployment

The target bridges for this project are two existing reinforced concrete girder bridges with 20-meter and 33-meter span length, respectively. Both bridges have 12-meter width and 0.2-meter thickness alphalt concrete slab, which is divided into 2 traffic lanes. In both bridges, there are 5 main girders with the transverse spacing of 2.3 meters. The main girders are connected by 3 cross beams in bridge #1 and 4 cross beams in bridge #2. The bridges have simply-suported boundary condition. From visual inspection, bridge #1 has 5-I girder cross section with medium surface condition and high traffic volume. The second bridge includes 5-I girder cross section with severe roughness damage and lower traffic volume. Figs. 4.1 and 4.2 present the inspection pictures of bearing, main girder, and surface condition in two existing bridges. The two test bed structures represent for the most typical short span existing bridges which were in service for more than 20 years. Two existing bridges were also constructed accoding to different standard specifications. The first bridge is constructed according to Vietnamese standard 22TCN 18-79. The second test bed structure followed AASHTO LRFD [1] in design stage. The designed load of two bridge are HS20-44 and H30-XB80, respectively. The general information of the structure type, traffic and roughness condition of two bridges are shown in Table 4.1. The cross sections of two existing bridges are presented in Fig. 4.4.

(a) Bearing

(b) Main girders

(c) Surface rougness

Figure 4.1: Current condition of bridge #1

(a) Bearing

(b) Main girders

(c) Surface roughness

Figure 4.2: Current condition of bridge #2

Table 4.1: Bridges information

Information	**Bridge #1**	**Bridge #2**
Bridge length (m)	20	33
Bridge width (m)	12	12
No of lanes	2	2
Girder type	I girder	T girder
Surface type	Asphalt Concrete	Asphalt Concrete
Surface condition	Moderate	Very poor
Traffic condition	High volume	Medium volume
Vehicle types	Car, truck, trailer	Car, truck, trailer
Designed load	1.25HS20-44	H30-XB80
Specification	AASHTO	22TCN18-1979
Year	2002	1997

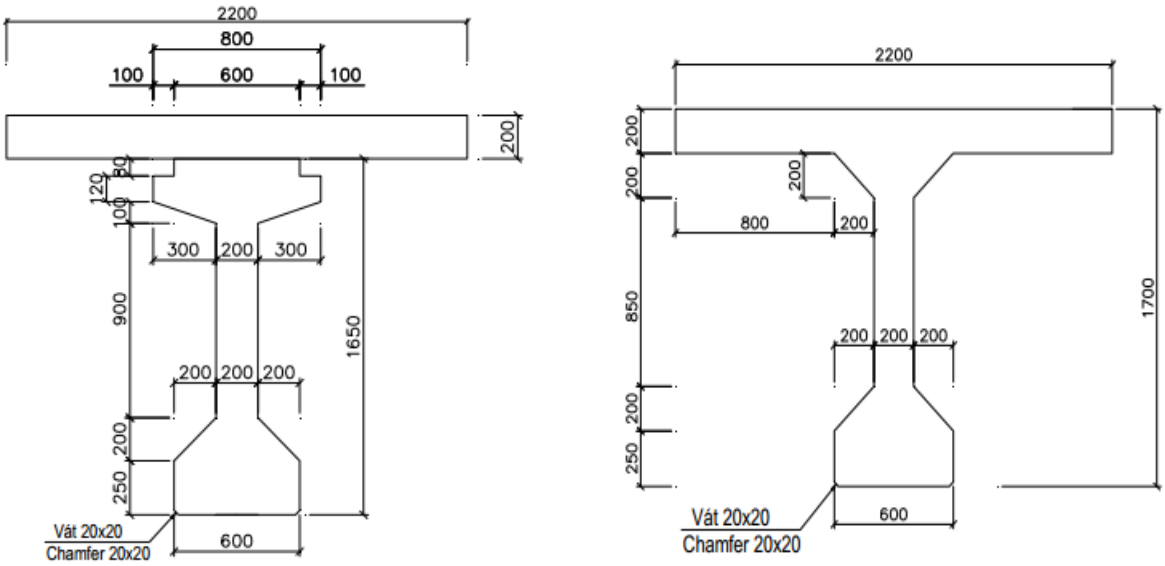

(a) I- girder cross section in bridge #1 (b) T-girder cross section in bridge #2

Figure 4.3: Cross section of two existing bridges

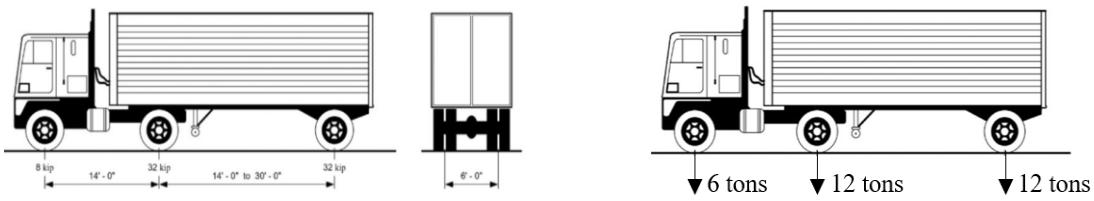

(a) Bridge #1: HS20-44 loading (b) Bridge #2: H30-XB80 loading

Figure 4.4: Design loading in two existing bridges

4.1.2 Data acquisition and traffic flow monitoring

To apply the time history analysis, the traffic data, bridge response and surface roughness condition of two target existing bridges are measured. Two Epson sensor nodes are attached near to the railing on the bridge for bridge acceleration monitoring. The sensors capture the acceleration data every 0.005 second with 20 Hz low pass filter for reducing noise. Two Epson sensors are synchronized by Bluetooth system via the measurement PC. The sensor has the measurement range of ±5G, 0.5 μ Grms/√Hz noise level, and 0.06 μ G/LSB. Fig.4.5 presents two sets of sensor deployment and measurement devices in two bridges. In the first configuration, two Epson sensors are deployed at the middle of bridge to investigate the shift of bridge response due to traffic volume. The sensors are then set at the quarter and middle of bridge to extract the bridge mode shapes and frequencies (Fig. 4.6)

At the same time, current traffic flow data is monitored via two cameras set on two lanes of the bridges. The traffic flow condition is characterized by traffic volume, which is the number of vehicles passing through a specific section in a specific time interval. To simplify the vehicle variation, traffic types are classified only as car and truck. During the data acquisition period, the number of car and truck passing through the bridge is counted every 5 minutes. On each bridge, 6 sets of both 5-minute acceleration data and traffic counting are collected. Fig. 4.7 shows the time history accelerations measured from sensor 1 and 2 in two existing bridges. At both lanes of the bridges, the measured accelerations are only slightly different between two sensors. The figures reveal that under real traffic excitation, maximum acceleration could reach to a very high value of 80 (gal) when heavy trucks pass through the bridges. For all measurement sets, the recorded response data are almost the same at both sensors. Tables 4.2 and 4.3 present the traffic volume counted on test bed structures.

The plots of traffic volume and RMS of vertical acceleration in 6 sets data at two lanes of the bridges are presented on Figs. 4.8 and 4.9. It is seen that in both test-bed structures, the number of trucks almost higher or equal to the number of cars, causing high bridge excitation responses. The measured traffic data and bridge responses will be used for creating the input force of traffic in time history analysis.

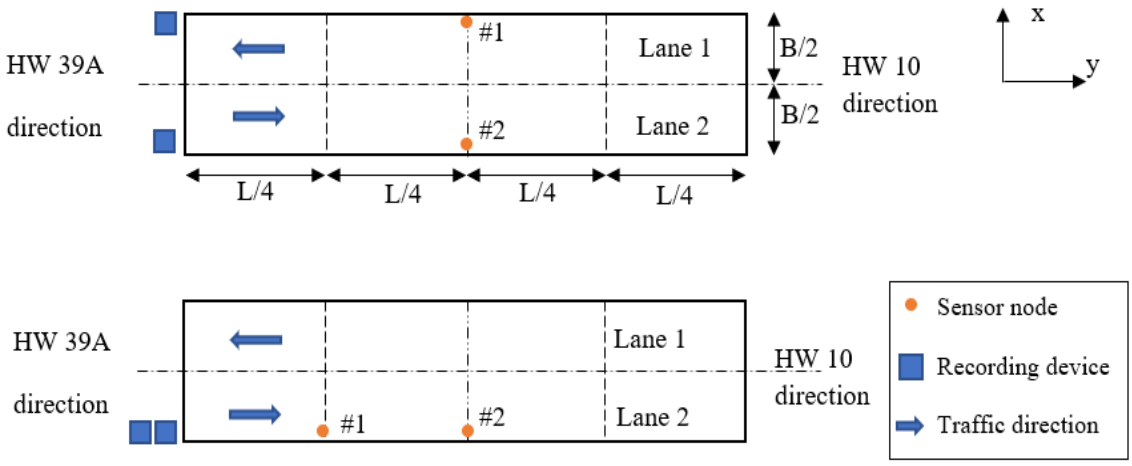

Figure 4.5: Sensor deployment in two existing bridges

(a) Sensor node (b) Data processing system (c) Connecting cable

Figure 4.6: Epson sensor components

The results show that the number of vehicles passing through bridge #1 are two times higher than bridge #1, however, the percentages of truck in both structures are almost the same. The highest truck ratio in two bridges are 71.8 % and 50 %, respectively. The comparative time history accelerations of both bridges in Fig. 4.7 shows that the maximum bridge dynamic response independence of truck ratio. The plots of vehicle number in 6 sets data at two lanes bridge #1 and #2 are presented on Fig. 4.8. It is seen that the number of trucks almost higher or equal to the number of cars, causing high bridge excitation responses. The RMS of vertical acceleration is also presented in Fig. 4.9.

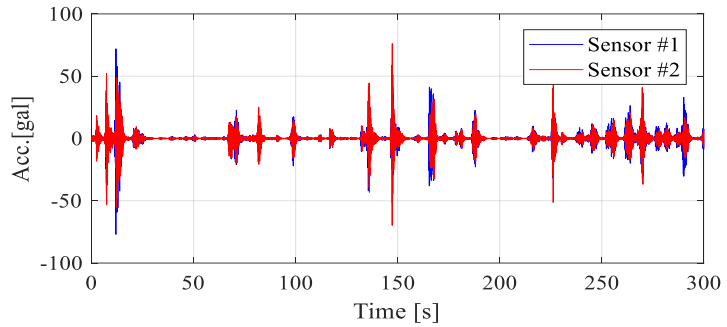

(a) Bridge #1 (set 1)

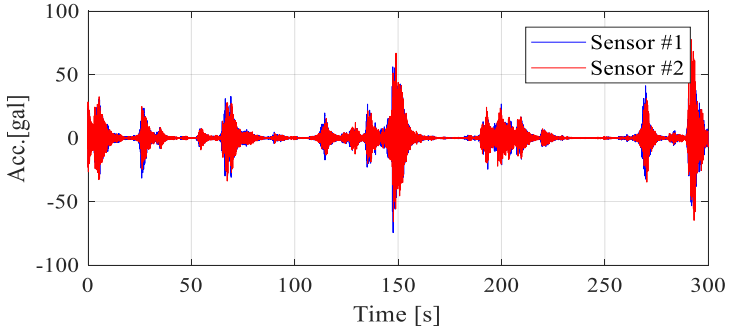

(b) Bridge #2 (set 1)

Figure 4.7: Time history of vertical acceleration in two existing bridges

Table 4.2: Traffic volume in bridge #1

Set	Car	Truck	Total	Truck ratio
1	47	32	79	40.5%
2	24	46	70	65.7%
3	21	41	62	66.1%
4	41	17	58	29.3%
5	12	36	48	71.8%
6	27	52	79	60.5%

Table 4.3: Traffic volume in bridge #2

Set	Car	Truck	Total	Truck ratio
1	19	16	35	45.7%
2	14	12	26	46.1%
3	18	18	36	50 %
4	13	6	19	31.5 %
5	14	14	28	50 %
6	16	9	25	36 %

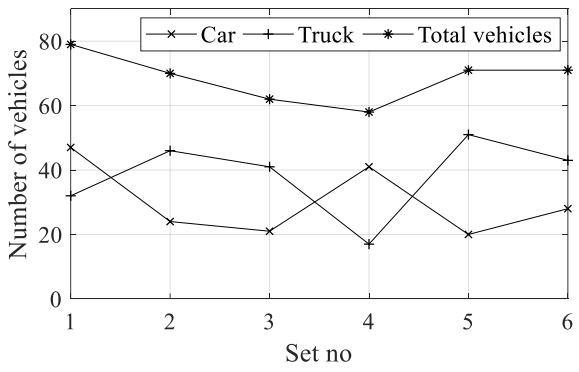

(a) Bridge #1

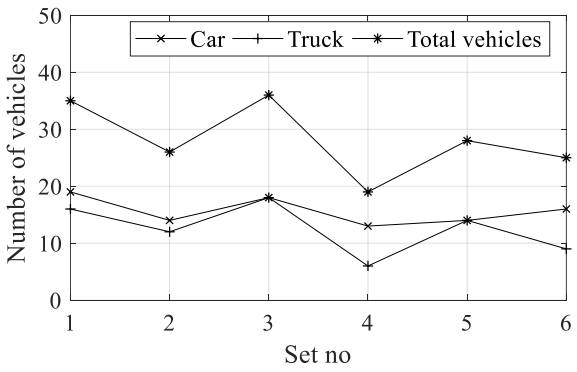

(b) Bridge #2

Figure 4.8: Traffic volume in two existing bridges

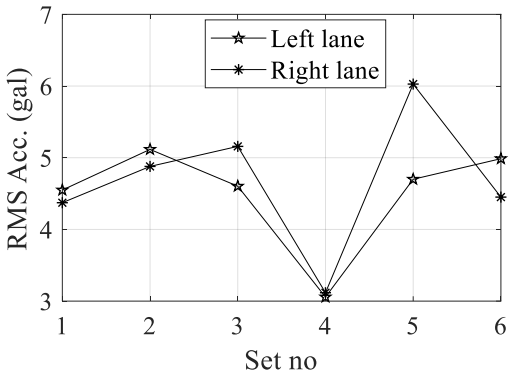

(b) Bridge #1

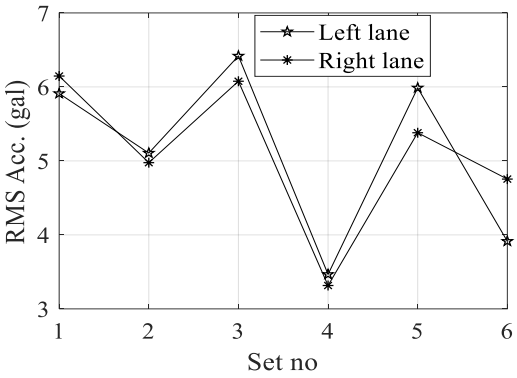

(b) Bridge #2

Figure 4.9: RMS of vertical acceleration in two existing bridges

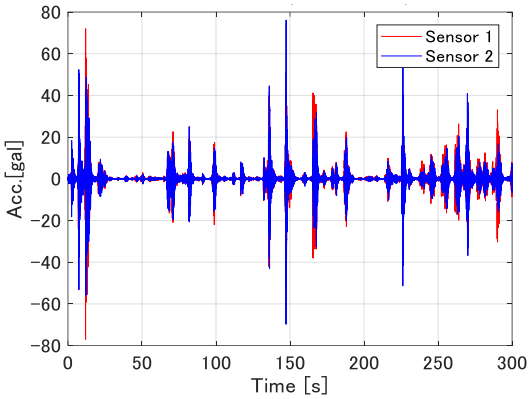

(a) Minimum truck ratio (set 4)

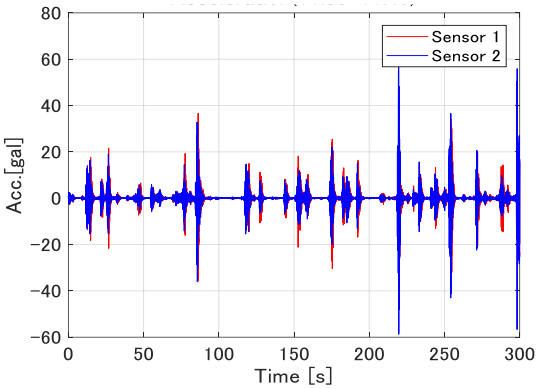

(b) Maximum truck ratio (set 5)

Figure 4.10: Time history of mid span deck vertical acceleration of bridge #1

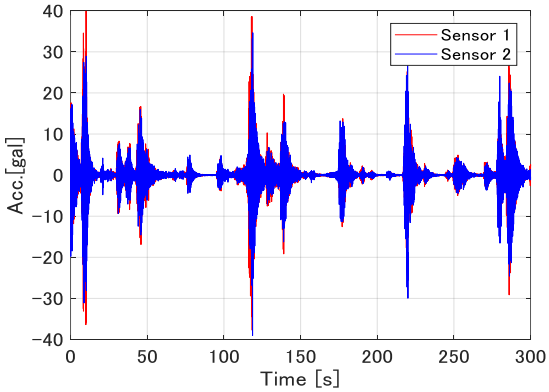

(a) Minimum truck ratio (set 4)

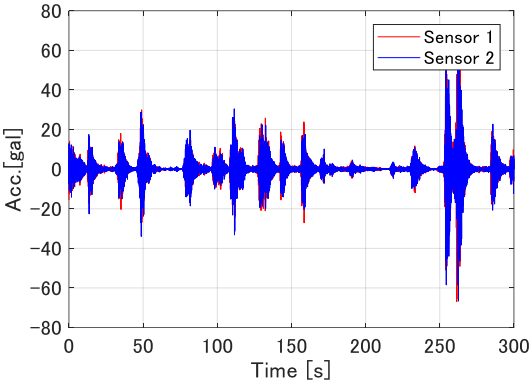

(b) Maximum truck ratio (set 3)

Figure 4.11: Time history of mid span deck vertical acceleration of bridge #2

Among measurement data sets, time history plots of maximum and minimum truck ratio and traffic volume of two bridges are presented in Figs. 4.10 and 4.11. According to the results, it is difficult to distinguish the traffic flow condition only from time history plot. Therefore, the power spectrum density (PSD) of bridge responses are presented in Figs. 4.12 and 4.13. Both bridges show the same peak of measured frequency in case of and minimum and maximum truck ratio. The 5-minute length vertical acceleration data in from sensor #1 attached left lane is sampled with 200 Hz frequency. Hanning window with overlap of 50% is applied in PSD calculation. The results show that both truck ratio conditions provide the same measured frequency.

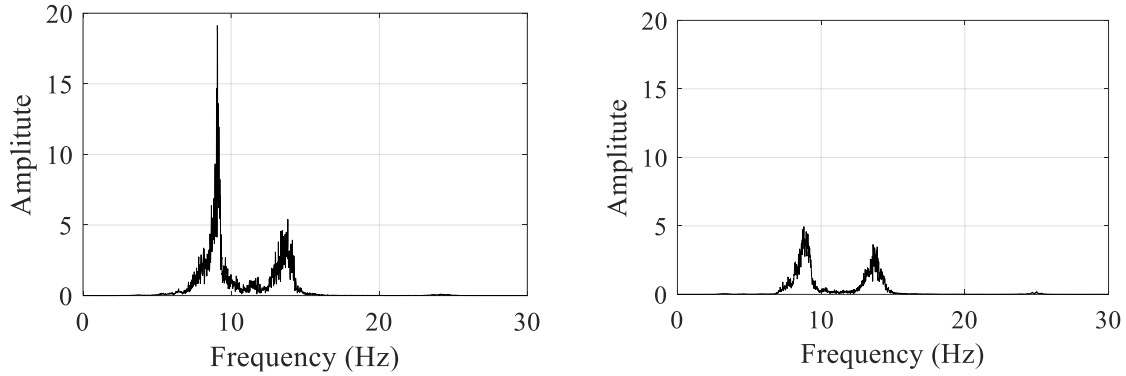

(a) Minimum truck ratio (set 4) (b) Maximum truck ratio (set 5)

Figure 4.12: Power spectrum density of bridge #1

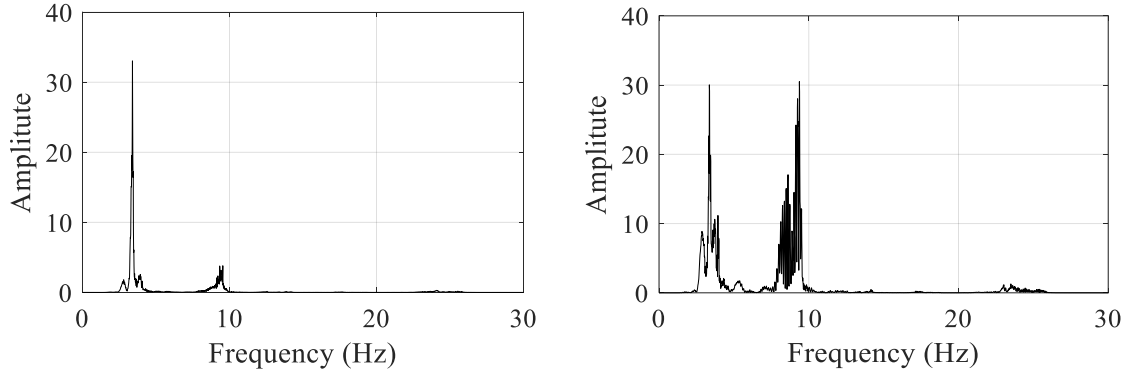

(a) Minimum truck ratio (set 4) (b) Maximum truck ratio (set 3)

Figure 4.13: Power spectrum density of bridge #2

To apply the time history analysis, the FE model of the target structures are constructed based on the designed document and inspection data. The built in FE model are validated by comparing the calculated mode shapes with measured frequencies extracted from PSD plot.

4.2 Bridge FE model validation

4.2.1 Bridge FE model

The finite element model of two existing bridges are constructed in Midas civil 2015. In both bridges, the main girder and cross beam are modelled as the beam element meanwhile the asphalt concrete slab is represented by plate element. The dimension of cross beams and main girders are designed as the provided document and by the inspection data. Both bridges have simply supported boundary condition at the two ends of the main girders. The concrete material has the compressive strength of 40 MPa with Young modulus of 3.39×10^7 kN/m^2 and 0.3 Poisson ratio. The density of concrete girder and slab are 25 kN/m^3 and 24 kN/m^3, respectively. FE model of bridge #1 includes 112 beam elements and 80 plate elements. Bridge #2 is constructed from 181 beam elements and 132 plate elements. From the eigen value analysis in Midas civil, the calculated mode shapes in two existing bridges are calculated. Figs. 4.14 and 4.15 presents the resulted mode shapes in FE model of bridges #1 and #2.

a) 1st mode: 8.82 Hz (b) 2nd mode: 10.29Hz (c) 3rd mode: 14.99 Hz (d) 4th mode: 22.73 Hz

Figure 4.14: Mode shapes in FE model of bridge #1

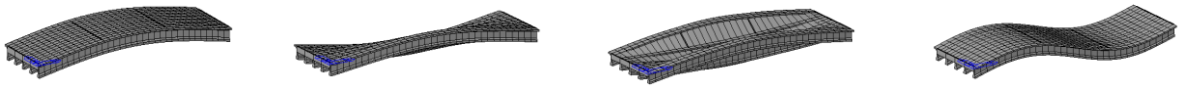

a) 1st mode: 3.14 Hz (b) 2nd mode: 4.23Hz (c) 3rd mode: 10.28 Hz (d) 4th mode: 12.10 Hz

Figure 4.15: Mode shapes in FE model of bridge #2

4.2.2 FE model validation

To validate the calculated mode shape in FE model, PSD of bridge frequency is calculated from measured data. The 5-minute acceleration data is divided into four segments with applied

Hanning window and 50% overlap. The sampling frequency for analysis is 200Hz. The PSD results show that, there are two main frequency ranges around 9.08 Hz and 13.46 Hz appear in all the acceleration cases of bridge #1. On the other hand, the frequencies appear in PSD plot of Nguyen bridge are around 3.34 Hz and 9.30 Hz for all three cases. Tables 4.4 and 4.5 presents the comparison results of calculated modes shapes in FE model and measured frequencies in two existing bridges. The discrepancies within 6% and 12% of in the first and third frequency ranges are found in both bridges. The FE model are validated and can be used for time history analysis.

Table 4.4: Measured frequency of bridge #1

Mode no.	FE model (Hz)	Measurement (Hz)
1st	8.82	9.08
2nd	10.29	-
3rd	14.99	13.46
4th	22.73	-

Table 4.5: Measured frequency of bridge #2

Mode no.	FE model (Hz)	Measurement (Hz)
1st	3.14	3.34
2nd	4.23	-
3rd	10.28	9.30
4th	12.10	-

4.3 Surface roughness condition

4.3.1 Surface roughness condition measurement

Nowadays, International roughness index (IRI) is one of the most common roughness indicators for bridge and road surface due to it dynamic and flexible application. In theory, IRI is defined as the accumulation of the un-sprung mass and sprung mass displacement over the length of the road profile [67]. Therefore, the roughness index has the unit of slop (mm/m or m/km). The value has been developed by World Bank in 1986 from previous research of National Cooperative Highway Research Program *(*NCHRP). It then has been widely applied in most of the countries in the word. In this project, Hawkeye DUO 1000 equipment is used for measuring IRI in both existing bridges. The IRI is calculated every 1-meter length to represent the local damage of the existing bridge. The Hawkeye 1000 Duo consists of a dual laser profiler and a single dashboard mounted video camera, which enables the collection of longitudinal

profile, roughness and macro-texture data, whist providing fully linked video images. Moreover, during the measurement, an GPS equipment attached on the vehicle for recording its position and velocity. The vehicle speed is controlled at 30 kilometres per hour. Fig. 4.16 presents the component of laser profiler in IRI measurement. Since the IRI only perform the road roughness in 2D dimension, the surface roughness condition in two vehicle lanes are measured to include the irregular surface in transverse direction.

(a) GPS (b) Laser (c) PC (d) Data acquisition

Figure 4.16: IRI devices

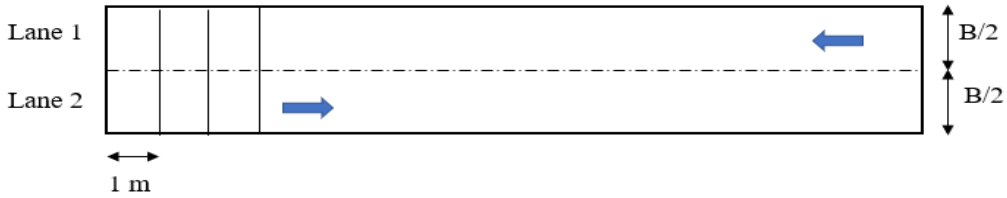

Figure 4.17: The arrangement of IRI load in two lanes

0	1	2	3	4	5	6	7	8	9	10	11	12	13	14	15	16	17	18	19	20
	7.70	4.67	3.19	3.30	4.60	5.19	4.05	5.84	5.48	2.15	3.05	3.28	2.09	1.45	2.73	1.26	9.00	9.21	9.69	5.25
	2.25	2.19	1.27	3.16	6.54	2.53	1.58	4.37	3.76	4.52	5.84	5.17	5.93	1.65	2.91	6.17	8.57	6.80	6.08	2.11

IRI < 3.1 3.1< IRI < 6.3 6.3< IRI < 12.5 12.5<IRI< 25 IRI>25

(a) IRI in every 1-meter segme

(b) Surface roughness from left side (c) Surface roughness from right side

Figure 4.18: IRI result at every 1- meter segment of bridge #1

The resolution of IRI value is 0.05 m. To ensure the result stability, the car runs 3 times on each lane and the IRI value is averagely calculated (Fig 4.17). The IRI value in each segment indicated the local damage positions which could amplify the dynamic vehicular load of vehicles passing through the bridges. Previous studies found that this local irregular roughness will yield repeat amplified vehicle loads, resulting in more severe pavement deterioration. IRI result of the measurement in every 1-meter length of two target bridges as and the inspection pictures are shown in Figs. 4.18 and 4.19.

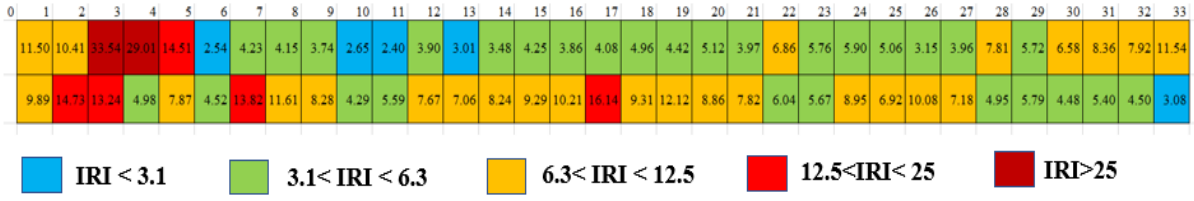

(a) IRI in every 1-meter segment

(b) Surface roughness from left side

(c) Surface roughness from right side

Figure 4.19: IRI result at every 1- meter segment of bridge #2

4.3.2 ISO road class from IRI

From the road class, we simulate the mean and COV of traffic total load due to roughness and vehicle. The statistical values will be used for building the dynamic load function level in time history analysis. According to the work of Kropáč [68] and Johannesson [69], the IRI can be converted to the PSD of road class in ISO 8608 by Eq. 4.1. Table 4.6 presents the value of IRI as respect to the PSD value and road class in ISO.

$$g_d(\Omega_0) = \left(\frac{IRI}{2.21}\right)^2 \tag{4.1}$$

The value of PSD represented for road roughness classification of each segment on bridge. Fig. 4.20 presents the bridge lane arrangement and road class results on two existing bridges. The results show that bridge #1 has average roughness condition meanwhile bridge #2 has significant damage surface. The level of local damage of roughness in each 1-meter bridge segment is classified from class A to E of ISO 8608. From the measured result, bridge #1 has more damage at the later end of the bridge, however, the transverse distribution of the damage in two traffic lanes is the same. On the other hand, bridge #2 has more severe damage roughness in the right lane as compared to the left lane.

Table 4.6: ISO 8608 and corresponding IRI value

Road class	$G_d(n_0)$		$G_d(\Omega_0)$		IRI
	Lower limit	Upper limit	Lower limit	Upper limit	
A	-	32	-	2	3.1
B	32	128	2	8	6.3
C	128	512	8	32	12.5
D	512	2048	32	128	25
E	2048	8192	128	512	50
F	8192	32768	512	2048	100
G	32768	131072	2048	8192	200
H	131072	-	8192	-	

In previous literatures, the 2D roughness level effect on bridge are investigated in some studies [70; 71]. It incorporates the multiple roughness in transverse direction of the bridge, however, the parallel roughness conditions are correlated to each other. Those work pointed out that the difference between the transverse surface roughness significant influence on bridge dynamic impact factor. In this study, the different distribution of measured local surface damage could cause the variability of vehicular dynamic load effect on existing bridges.

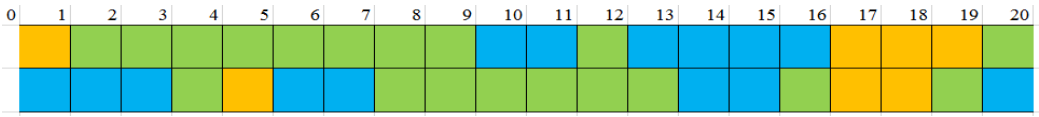

(a) Bridge #1

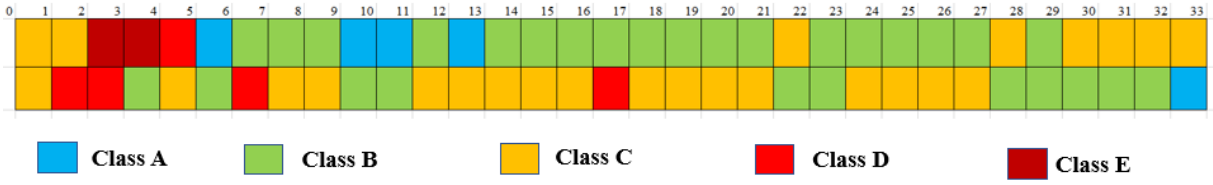

(b) Bridge #2

Figure 4.20: The converted ISO road class at every 1-meter bridge segment

In this section, bridge dynamic measurement and traffic counting are implemented in two existing bridges in Vietnam. The traffics pass through both bridges have more than 50% truck ratio, causing high acceleration on deck slab. The basic frequencies of the bridges under traffic excitation are then obtained by power spectrum density method of two sensors located at the middle and the quarter of the bridges. The calculated results mode shapes have the good agreement with the measured frequencies, therefore the FE model of the target bridges are validated. The constructed FE model will be used for time history analysis to evaluate the bridge dynamic response. The IRI measurement results provide useful information of the local surface damages on bridge where the dynamic wheel loads are amplified.

4.4 Effect of local surface irregularity on bridge dynamic responses

This section presents the procedure of creating the input traffic load in time history analysis with considering the effect of local roughness damage. Firstly, the measured traffic volume data will be used for constructing the traffic flow. The vehicles in traffic volume will be run with random passing orders and constant speed. The headway time between two consecutive vehicles is calculated from given traffic volume and speed. Each axle of traffic vehicle is represented by the forcing function with fluctuated amplitudes. The amplitude of vehicle variate according to the vehicle types and roughness condition. A quarter car model simulation is implemented to calculate the mean and COV of total load of vehicle with respect to roughness condition. The result statistical values are used to randomly generate the amplitude of traffic force function. Finally, the input force of the whole traffic flow is assigned at each

discretized node in bridge FE model. Each node represented for the local condition of roughness, therefore, the variation level of force amplitude will be change. Time history analysis are implemented to evaluate the effect of local roughness damage on bridge dynamic responses.

4.4.1 Construction of input traffic load

To evaluate the vehicular force amplified by local surface roughness damage, vehicle roughness simulation is implemented for every 1- meter segment. The car and truck are represented as quarter car model with specific parameters. In IRI measurement, the IRI values of every 1-meter segment length are converted to PSD of the road class from A to E in ISO 8608 classification. The roughness profile of road class is generated according to the literature. The wave length of the generated profile is from 0.02 m to 1 m. Fig. 4.21 show the profile plot and PSD of generated profile A to E of 1 –meter bridge segment.

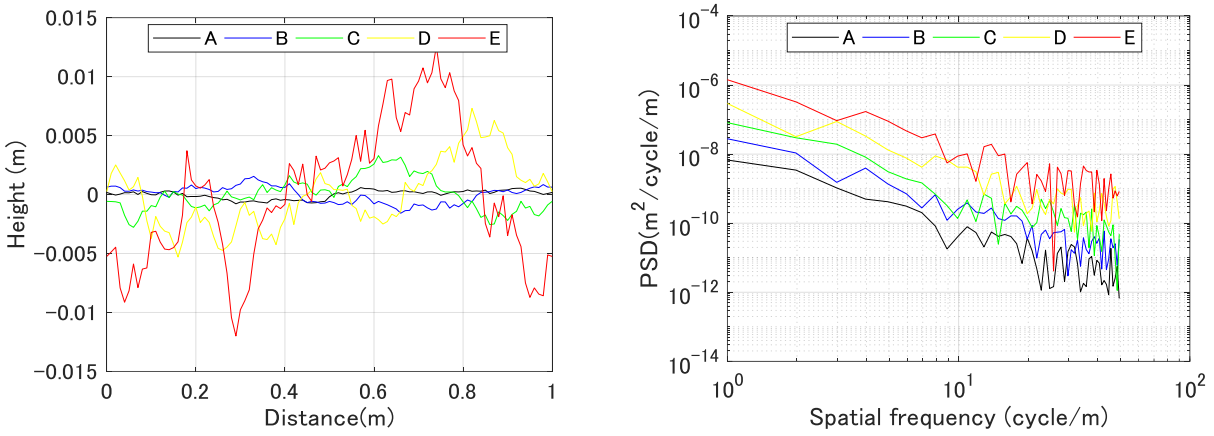

(a) Roughness profile (b) PSD of profiles

Figure 4.21: The generated profile for 1-meter bridge segment

By solving equation of motion of quarter model, the fluctuated dynamic load P_{dyn} of each vehicle type on surface profile is calculated as Eq. 3.4. The total load of vehicle P_{total} is the summation of fluctuated dynamic load and the static load $(m_u+m_s)g$ of vehicle (Eq.3.5). Detail of the quarter car simulation was already presented in detail in Chapter 3.

$$P_{dyn} = k_t\left(h - y_1\right) \tag{3.4}$$

$$P_{total} = P_{dyn} + \left(m_u + m_s\right)g \tag{3.5}$$

To characterize the randomness of the total load, the mean and COV of total load under road profile A to E are calculated in every 1-meter span length. For each ISO road level, 100

profiles are generated to reduce the bias of the random roughness profiles. The average values of mean and COV of total load are then calculated to reduce the bias of roughness. According to the measurement data, the traffic vehicle has speed of 30 km/h. Fig. 4.22 shows the standard error bar of the total load of car and truck in 1-meter segment length in ISO road class A to E with the speed of 30 km/h. The results show that as the roughness condition deteriorated, the mean of total load of vehicle fluctuates. The variation of the COV of total load of car and truck is also plotted in Fig. 4.23. The figure shows that COV value increase with the damage of road profile. The values do not fluctuate much at road class A but they significantly variate at class E. The COV values even reach to 18% and 28% for car and truck respectively at this ISO road class. It can be concluded that the roughness condition contributes the most in the variation of total of vehicle. The value of mean and COV of total load of car and truck will be used to generate the amplitude of input load forcing function in time history analysis.

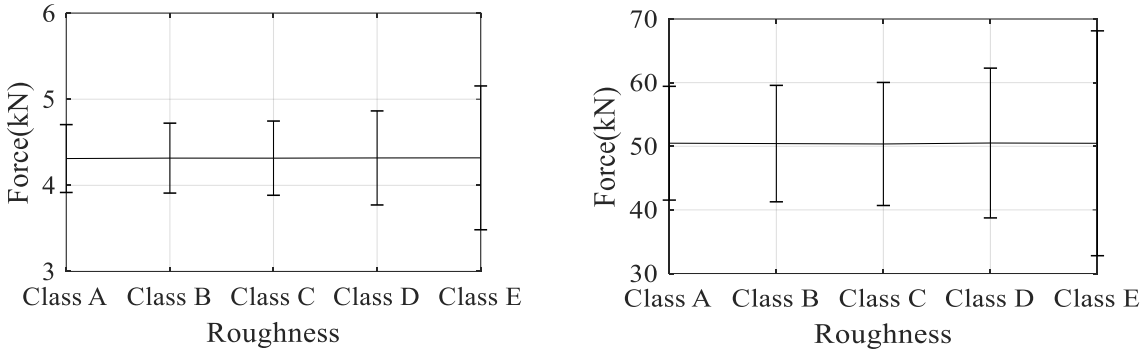

(a) Car (b) Truck

Figure 4.22: Error bar of mean total load of car and truck in different roughness (v=30 km/h)

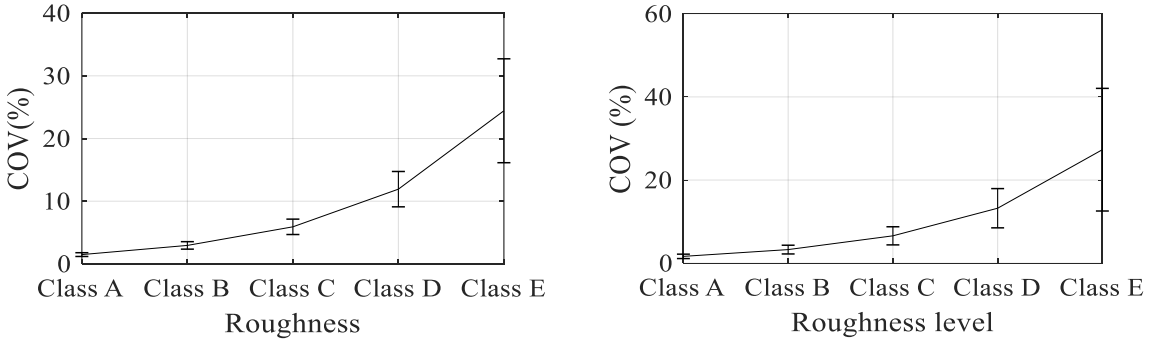

(a) Car (b) Truck

Figure 4.23: Error bar of COV of car and truck in different roughness (v=30 km/h)

4.4.2 Validation of numerical scheme

In both bridges, 6 sets of traffic monitoring data and mid-span deck acceleration are recorded at the left and right lane of the bridges. To validate the scheme in two existing bridges, time history analysis is implemented in all 6 sets of traffic condition. The input traffic force is constructed from the traffic volume of each vehicle types, car and truck pass though the bridge at two lanes of the bridge. The target bridge includes 5 main girders which are numbered from girder #1 to girder #5 from left to right lane. Assume that the vehicles always run at the middle of bridge lanes with opposite direction, the traffic flow is assigned at girder 2 (left lane) and girder 4 (right lane) respectively. For each traffic set, 10 random passing orders of traffic vehicles are generated. The calculated acceleration is averaged value of 10 different passing orders. The vehicle runs with speed of 30 km/h.

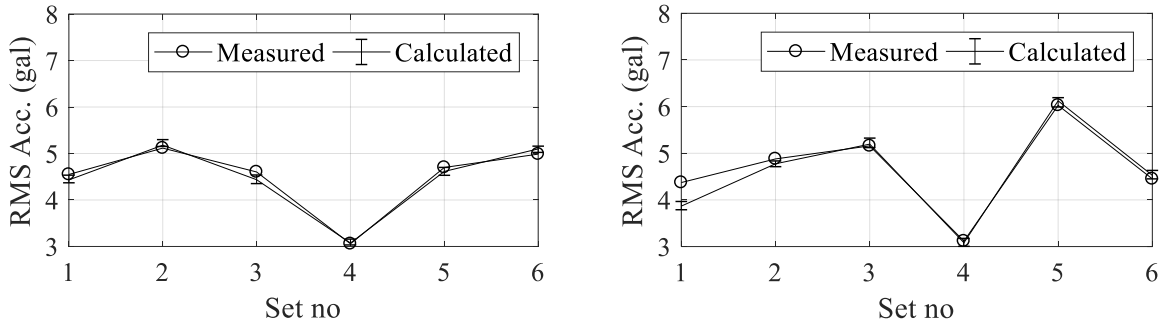

(a) RMS Acceleration-left lane (b) RMS Acceleration- right lane

Figure 4.24: Validation of bridge #1

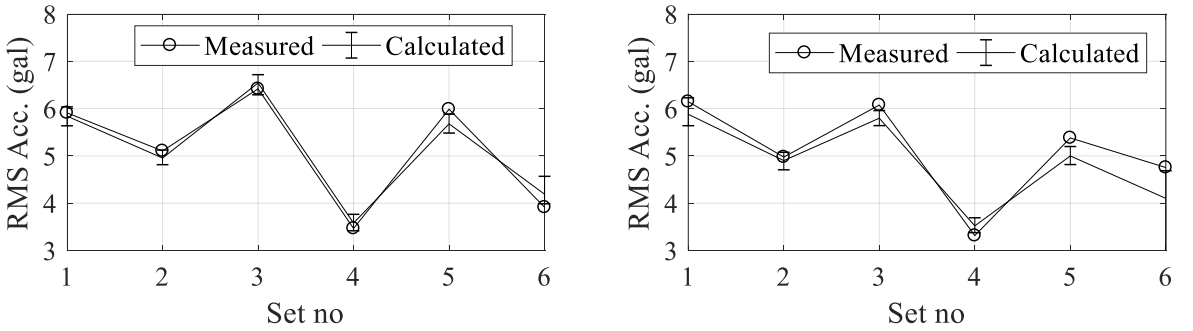

(a) RMS Acceleration-left lane (b) RMS Acceleration- right lane

Figure 4.25: Validation of bridge #2

Figs. 4.24 and 4.25 present the comparison of RMS measured and maximum, minimum error bar of calculated acceleration in left and right lane of two existing bridges. The results show that the calculated acceleration among 6 sets of traffic has good agreement with the measured data in both bridges. Therefore, the scheme can further be applied for investigate the effect of local roughness damage on bridge dynamic responses in the next section.

4.4.3 Effect of local roughness damage and traffic passing orders

To investigate the effect of local damage on the dynamic response of two bridges, the time history analysis is implemented with the same traffic condition in case of random good, average, bad roughness and with the different local damage roughness conditions. The chosen traffic conditions in bridge #1 and #2 have 71.8 % (set 5) and 50% truck ratio (set 3) respectively. The calculated mean of RMS acceleration at mid span of bridge under ten random passing orders of the given traffic flow represent for statistical characteristic of bridge dynamic response. Assume that the traffic vehicle run on the middle of girder #2 (left lance) and girder #4 (right lane) in opposite direction. The constructed traffic flow on bridge travel with 30 km/h velocity, as provided in the monitoring data. According to LRFR code, the dynamic impact factor IM changes slightly from 0.1 in smooth surface to 0.2 in minor surface damage, and 0.33 for the other cases. Those surface conditions could be assumed as good roughness (class A), average roughness condition (class B), and bad roughness (class E). Therefore, time history analysis is implemented with above surface conditions. Fig. 4.26 shows the roughness condition of class A, B, and E in bridge #1.

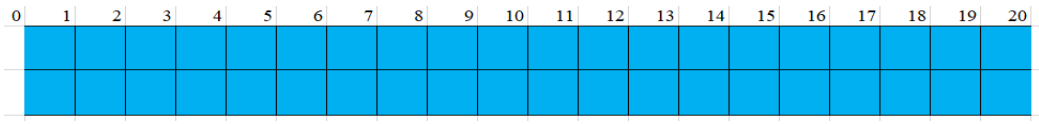

(a) Class A

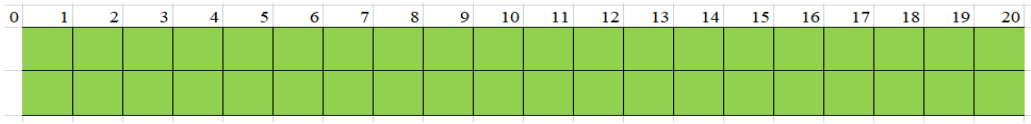

(b) Class B

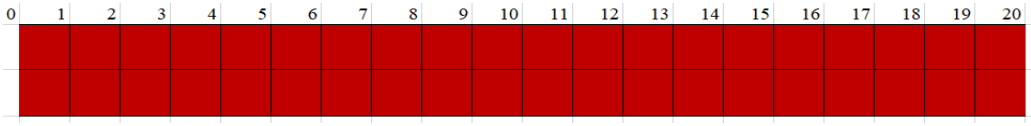

(c) Class C

Figure 4.26: Local damage of surface condition on bridge #1

The ratio between RMS of acceleration in different roughness condition case and the good condition are calculated in girder #1, as represented by α in Eq. 4.2:

$$\alpha = \frac{\text{RMS Acc.(condition } i\text{)}}{\text{RMS Acc.(class A)}} \tag{4.2}$$

Where α represents for the dynamic increment due to both traffic condition and roughnesss condition on existing bridges. The average value of α in 5 passing orders in bridge #1 and #2 with respect to the provided IM in LRFR codes at class A, class B, and class E are presented in Fig. 4.27.

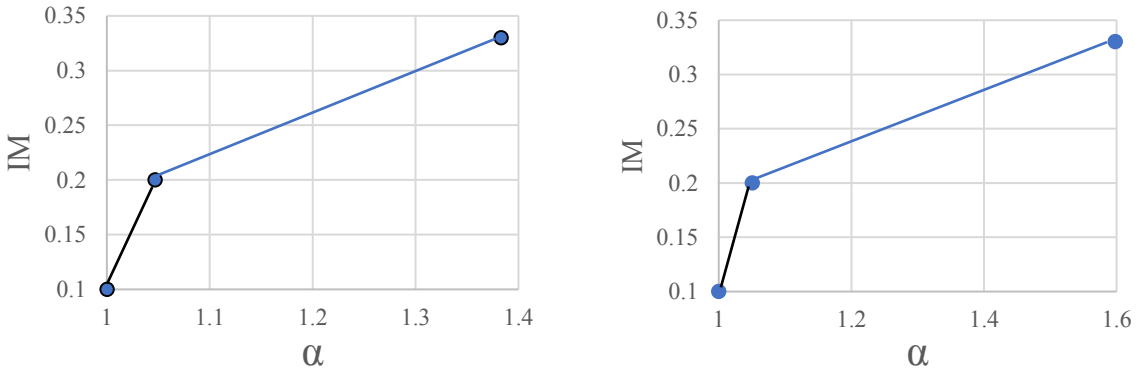

(a) Plot of IM and α in bridge #1 (b) Plot of IM and α in bridge #2

Figure 4.27: Relation of IM and α in two existing bridges

It should be noted that, LRFR code for bridge rating provided the value of dynamic impact factor in random roughness condition, however, the value of IM at local damage surface was not yet considered. From three points of the plot in Fig. 4.27, the relationship between IM and α could be calculated as Eq. 4.3 and 4.4. Therefore, the value of IM under different roughness conditions and given traffic flow, including local damage could be expressed in term of α :

$$IM_{1a} = 2.1395\alpha - 2.0395 \tag{4.3a}$$

$$IM_{1b} = 0.3864\alpha - 0.2045 \tag{4.3b}$$

$$IM_{2a} = 1.9882\alpha - 1.882 \tag{4.4a}$$

$$IM_{2b} = 0.2372\alpha - 0.0491 \tag{4.4b}$$

The value of α at current conditions and some possible local damage conditions are calculated in two existing bridges. Based on the current condition, assume that the local surface

damage could develop at the last quarter end of bridge deck in bridge #1. Meanwhile, the damage is expanded at the first quarter, middle, and final quarter of bridge #2. Figs. 4.28 and 4.29 present the detail of local roughness conditions in two existing bridges. The dynamic ratio α indicated that the local surface damage on existing bridge influences on the bridge dynamic response. The calculated values of α in simulation are substituted in the Eqs. 4.3(a-b) and 4.4(a-b) to calculate the dynamic impact factor IM in given local damage scenarios, as shown in Tables 4.7 and 4.8. The value of IM in all possible roughness is smaller than 0.33 which is indicated in LRFD code. The calculated IM in this research could be used for calibrating the IM in rating factor formula and to assess the condition of existing bridges under given traffic flow and local roughness condition at sides.

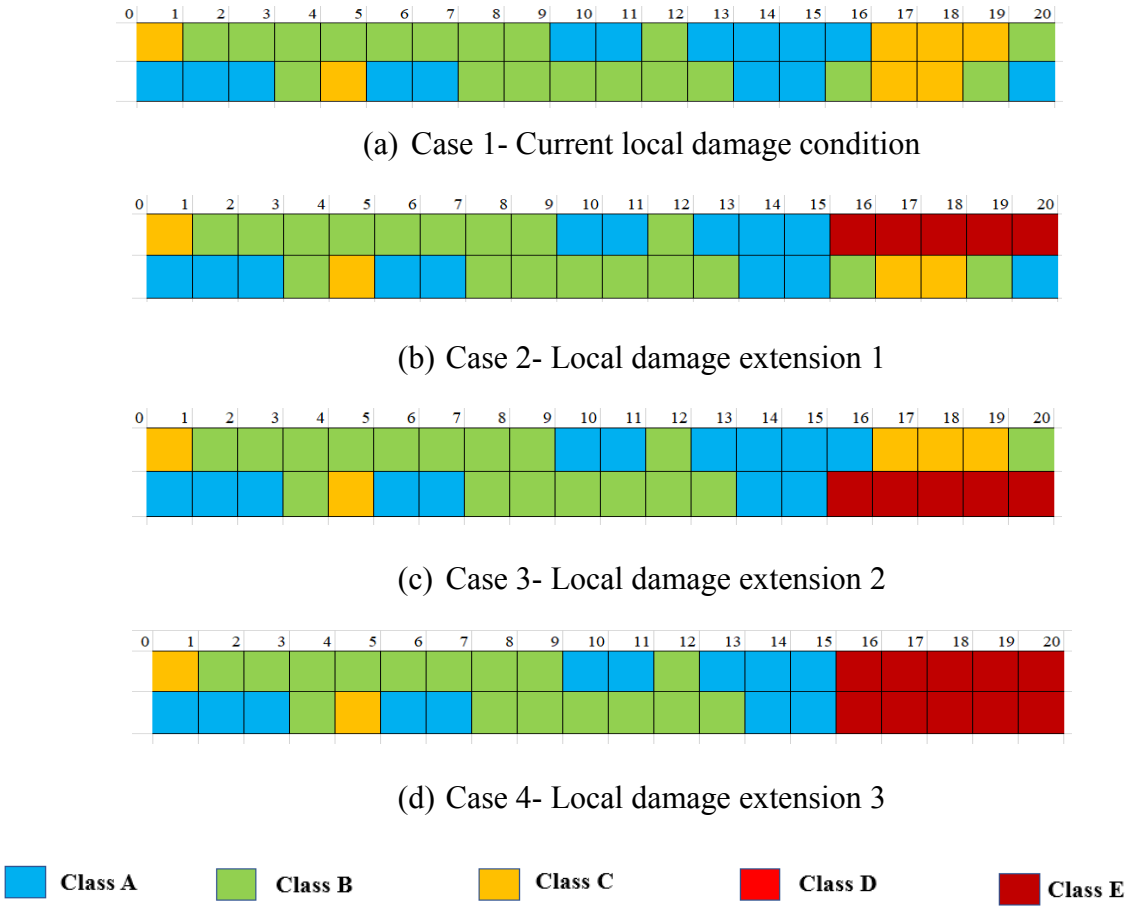

(a) Case 1- Current local damage condition

(b) Case 2- Local damage extension 1

(c) Case 3- Local damage extension 2

(d) Case 4- Local damage extension 3

Figure 4.28: Local damage of surface condition on bridge #1

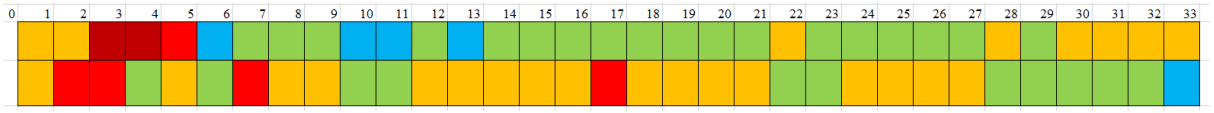

(a) Case 1-Current local damage condition

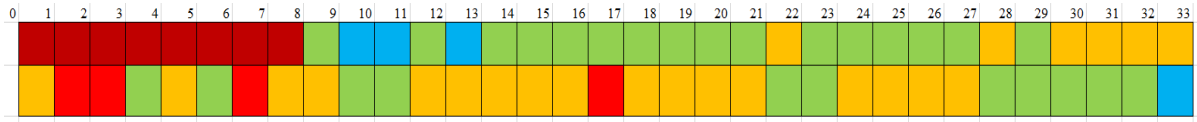

(b) Case 2- Local damage extension 1

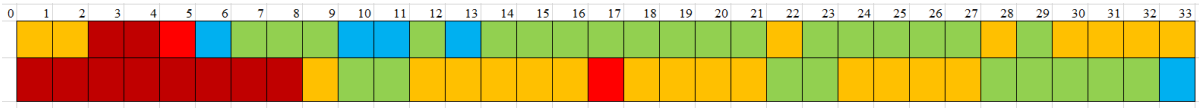

(c) Case 3- Local damage extension 2

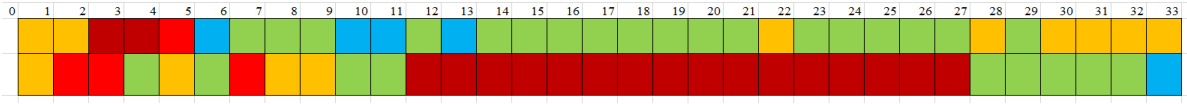

(d) Case 4- Local damage extension 3

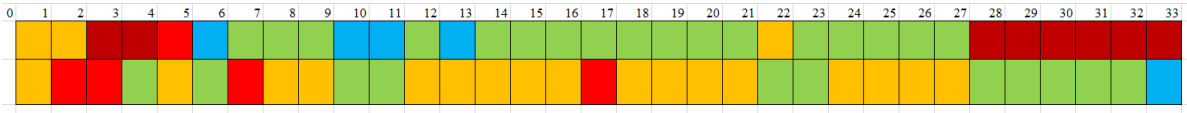

(e) Case 5- Local damage extension 4

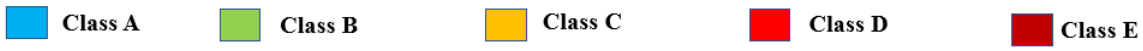

Figure 4.29: Local damage of surface condition on bridge #2

Table 4.7: IM in different local damage in bridge #1

Case	α	IM
1	1.02	0.136
2	1.08	0.212
3	1.02	0.136
4	1.08	0.212

Table 4.8: IM in different local damage in bridge #2

Case	α	IM
1	1.04	0.182
2	1.07	0.204
3	1.05	0.203
4	1.12	0.217
5	1.08	0.207

4.5 Summary

This chapter applies the proposed numerical scheme to investigate the dynamic load effect of traffic flow on two existing multiple reinforced concrete bridges. At first, traffic data, bridge dynamic response and roughness condition are measured to construct the input traffic load assigned at each discrete deck node on built in bridge FE model. Time history analysis is implemented on the target bridges considered effect of traffic flow and local roughness damage. Effect of vehicle passing orders and vehicle speed on the bridge dynamic responses at the same traffic condition and current surface roughness is also examined. From the results of numerical simulation, some conclusions can be summarized as below:

- The fluctuation of RMS acceleration agrees well with measured data
- The current condition of local damage increases the dynamic effect of traffic vehicles on bridges which is indicated by the value of α .
- From the plot of IM as indicated in LRFR and α , the function of IM from α is constructed
- The scheme proposed dynamic impact factor of given traffic flow and local surface damage condition which can be used for calculating rating factor and to assess the current condition of existing bridges.

Chapter 5

5. CONCLUDING REMARKS

The variation of vehicle types, speeds, and passing order in traffic flow and roughness conditions fluctuate the dynamic effect of vehicle dynamic load in the existing bridges and bridge dynamic response. This thesis proposes a numerical calculation scheme to evaluate the vehicle dynamic load effect on existing bridges considering traffic flow and surface roughness condition. Firstly, the general idea of the numerical scheme on bridge is introduced. The numerical scheme is validated on a target steel box girder bridge with measured traffic data and random roughness condition. Then, the investigation on effect of local roughness damage on bridge response is implemented in two existing bridges with deteriorated surface condition.

The first part of the thesis introduces the flow of calculation scheme applied to estimate dynamic effect on existing bridges considering traffic data and surface roughness. The steps to simulate traffic flow from traffic volume data with different vehicle types, speeds, and random passing order is described in detail. Traffic data and bridge acceleration are measured on the target structure. A validated FE model of the bridge constructed and validated with the

measurement data for time history analysis. From the given traffic data, the generated input traffic load considering the effect of roughness condition is constructed. Finally, time history analysis is implemented in the available Midas Civil software to evaluate bridge dynamic responses.

In the second part, validation of the proposed numerical scheme is presented. At first, the parameters of target bridge, the dynamic data acquisition, and the traffic measurement are presented. The target structure for validating the numerical scheme is an existing steel box-girder bridge. The monitored traffic data are collected in term of traffic volume of each vehicle type in every 10 minutes. During the traffic monitoring, data acquisition is also conducted to extract the traffic patterns which influence on bridge dynamic responses. It was found that the RMS acceleration has positive correlation with the number of truck and truck ratio. Therefore, truck ratio, passing order, and vehicle speed are chosen as the traffic patterns for constructing the traffic flow. From the given traffic data, traffic flow with random passing order of vehicles are built. A constructed FE model of the test bed structure are validated by comparing the calculated and measured frequency in the bridge. To consider the effect of uncertainty of vehicle properties and random roughness on the fluctuated vehicular load, a quarter car model simulation is implemented. The mean and COV of total load of car and truck considering random vehicle suspension parameter, vehicle speeds, and roughness condition are calculated. It was found that the total load of vehicle is significantly influenced by roughness condition. The statistical values of total load are used to construct the transient time history loading function assigned on the deck node of the target bridge FE model. The variation of input load amplitude represents for the random vehicle types, speed and roughness condition. To validate the numerical scheme, the RMS accelerations under different truck ratio are compared with data acquisition results for time history analysis validation. Bridge dynamic response is calculated during 1- hour length traffic data with high and low traffic ratio. The high truck ratio traffic is from 8 am to 9 am at which the number of trucks accounted for approximate 20% of total vehicles. Meanwhile, truck ratio is lower than 10% from 6 pm to 7 pm. The calculation results show the showed agreements with that of the measurement data especially in the traffic situation with low truck ratio. The parametric study on effect of truck ratio, vehicle speed, vehicle passing orders and random surface roughness conditions on the bridge dynamic responses was implemented with the given results:

- The RMS acceleration increases with the increment of vehicle speed mean while it slightly changes from good to bad surface condition. At the same traffic condition and

speed, the RMS acceleration did not fluctuate among different passing orders of traffic vehicles.

- The variation of vehicle speed, vehicle passing order, and surface roughness condition influences on maximum of bridge acceleration. The value is independence of truck ratio; however, it is influenced by both speed and surface roughness condition. The maximum acceleration is also highly fluctuated by variation of vehicle passing order in traffic flow, especially at high speed and bad surface roughness.

Effect of local surface damage on bridge dynamic response is also investigated by using the proposed numerical scheme on the multiple reinforced concrete bridges girder with bad roughness condition. The mid-span deck acceleration and traffic volume are measured every 5 minutes. Bridge acceleration is measured in the middle and the quarter of the bridge. Total of 9 sets of results will be used to statistically evaluate the mean and standard deviation of bridge dynamic responses, number of vehicles and percentages of truck pass through the bridge. International roughness index (IRI) at every 1-meter length segment of bridge are measured by a laser equipment for bridge roughness condition. The level of local damage of roughness in each 1-meter bridge segment is classified from class A to E of ISO 8608. From the measured result, bridge #1 has more damage at the later end of the bridge, however, the transverse distribution of the damage in two traffic lanes is the same. On the other hand, bridge #2 has more severe damage roughness in the right lane as compared to the left lane. The same numerical scheme is applied on the target bridges to evaluate bridge dynamic response with considering traffic and local surface roughness. The acceleration caused by local roughness are compared with the value oscillated by good roughness condition. some conclusions can be summarized as below:

- The fluctuation of RMS acceleration agrees well with measured data
- The increment of vehicle dynamic effect considering traffic and local surface damage on existing bridges is indicated by ratio α of RMS acceleration in surface condition i and RMS acceleration in good surface condition. The relationship of IM and α are constructed.
- The scheme proposed reference dynamic impact factor of given traffic flow and local surface damage condition which can be used for calculating rating factor of existing bridges.

The proposed numerical scheme combines effect of traffic flow and surface roughness irregularity to evaluate vehicle dynamic load effect on existing bridges. Variation effect of vehicle speeds, passing orders, truck ratio, and roughness condition including random and local roughness condition on bridge dynamic response is investigated. The calculation scheme was applicable to evaluate vehicle dynamic load effect of existing bridges with the given dynamic monitoring data, traffic flow, and surface roughness condition.

This research mainly provided a numerical scheme to evaluate dynamic impact factor of bridge considering traffic flow and surface roughness condition. There are several recommendations for future researches could be listed below:

- In this study, the dynamic ratio α is calculated from the bridge acceleration of the middle girder. Due to the local damage, at some location of all girder where the surface is significantly deteriorated, bridge response may be amplified, leading to higher IM. Therefore, it is necessary to further calculate the dynamic allowance of all girder, especially at the severe damage locations.
- The study proposed the value of IM due to both current traffic flow and local roughness damage in existing bridge. If the current resistance of the structure could be inspected, the bridge rating could be estimated to evaluate the condition of existing bridges.

BIBLIOGRAPHY

[1]American Association of State Highway Officials (AASHTO). (2012). LRFD Bridge Design Specifications. In Washington, DC, USA.

[2]Hwang, E.-S., & Nowak, A. S. (1991). Simulation of dynamic load for bridges. Journal of Structural Engineering, 117(5), 1413-1434.

[3]American Association of State Highway Officials (AASHTO). (2011). Manual for bridge evaluation. In Washington. DC.

[4]Japan Road Association (JRA). (1996). Specifications for highway bridges. Part 1: Common specifications. In: Tokyo.

[5]New Zealand Transport Agency (NZTA). (2013). Bridge manual. In: Wellington, New Zealand.

[6]Canadian Standards Association (CSA). (2006). Canadian highway bridge design code. In: Mississauga, ON, Canada.

[7]Ministry of Transport of People 'S Republic Of China (MTPRC). (2004). General code for design of highway bridges and culverts. In: Beijing.

[8]European Committee For Standardization (CEN). (2003). Eurocode 1: Actions on structures—Part 2: Traffic loads on bridges. In: Brussels, Belgium.

[9]Austroads (AS). (2004). 5100: Bridge Design-part2: Design load. In. Sydney, Australia.

[10]Bristish Standard Institution (BSI). (2006). 5400-2. Steel, Concrete and Composite Bridges-Part 2: Specification for Loads. In: BSI: London, UK.

[11]Deng, L., & Cai, C. (2010). Development of dynamic impact factor for performance evaluation of existing multi-girder concrete bridges. Engineering Structures, 32(1), 21-31.

[12]Deng, L., Cai, C., & Barbato, M. (2011). Reliability-based dynamic load allowance for capacity rating of prestressed concrete girder bridges. Journal of Bridge Engineering, 16(6), 872-880.

[13]Mitchell, C., & Gyenes, L. (1989). Dynamic pavement loads measured for a variety of truck suspensions.'2nd Int. Conf. on Heavy Vehicle Weights and Dimensions, Kelowna. British Columbia.

[14]Deng, L., & Cai, C. (2010). Identification of dynamic vehicular axle loads: theory and simulations. Journal of Vibration and Control, 16(14), 2167-2194.

[15]Hahn, W. (1987). Effects of commercial vehicle design on road stress-vehicle research results. Report No.453.

[16]Cole, D., & Cebon, D. (1989). Simulation and measurement of dynamic tyre forces: Cambridge University Press.

[17]Potter, T., Cebon, D., Collop, A., & Cole, D. (1996). Road-damaging potential of measured dynamic tyre forces in mixed traffic. Proceedings of the Institution of Mechanical Engineers, Part D: Journal of Automobile Engineering, 210(3), 215-225.

[18]Pesterev, A., Bergman, L., & Tan, C. (2004). A novel approach to the calculation of pothole-induced contact forces in MDOF vehicle models. Journal of sound and vibration, 275(1-2), 127-149.

[19]Michaltsos, G. (2000). Parameters affecting the dynamic response of light (steel) bridges. Facta universitatis-series: Mechanics, Automatic Control and Robotics, 2(10), 1203-1218.

[20]OBrien, E., Li, Y., & González, A. (2006). Bridge roughness index as an indicator of bridge dynamic amplification. Computers & structures, 84(12), 759-769.

[21]Willis, R. (1849). Appendix to the Report of the Commissioners Appointed to Inquire into the Application of Iron to Railway Structures. Stationary Office, London.

[22]Timoshenko, S. (1922). CV. On the forced vibrations of bridges. The London, Edinburgh, and Dublin Philosophical Magazine and Journal of Science, 43(257), 1018-1019.

[23]L. Frýba. (1973). Vibration of Solids and Structures under Moving Loads. Zeitschrift Angewandte Mathematik und Mechanik, 53, 502-503.

[24]Henchi, K., Fafard, M., Dhatt, G., & Talbot, M. (1997). Dynamic behaviour of multi-span beams under moving loads. Journal of sound and vibration, 199(1), 33-50.

[25]Yang, Y.-B., Yau, J.-D., & Hsu, L.-C. (1997). Vibration of simple beams due to trains moving at high speeds. Engineering Structures, 19(11), 936-944.

[26]Darjani, S. (2013). Dynamic Response of Highway Bridges Under a Moving Truck and Development of a Rational Serviceability Requirement. New Jersey Institute of Technology, Department of Civil and Environmental Engineering.

[27]Ting, E., Genin, J., & Ginsberg, J. (1974). A general algorithm for moving mass problems. Journal of Sound Vibration, 33, 49-58.

[28]Akin, J. E., & Mofid, M. (1989). Numerical solution for response of beams with moving mass. Journal of Structural Engineering, 115(1), 120-131.

[29](Lee, H.). (1996). The dynamic response of a Timoshenko beam subjected to a moving mass. In: Elsevier.

[30]Esmailzadeh, E., & Ghorashi, M. (1997). Vibration analysis of a Timoshenko beam subjected to a travelling mass. Journal of sound and vibration, 199(4), 615-628.

[31]Yang, Y., & Lin, C. (2005). Vehicle–bridge interaction dynamics and potential applications. Journal of sound and vibration, 284(1-2), 205-226.

[32]Biggs, J. M., & Biggs, J. M. (1964). Introduction to structural dynamics: McGraw-Hill College.

[33]Yang, Y.-B., & Wu, Y.-S. (2001). A versatile element for analyzing vehicle–bridge interaction response. Engineering Structures, 23(5), 452-469.

[34]Pan, T.-C., & Li, J. (2002). Dynamic vehicle element method for transient response of coupled vehicle-structure systems. Journal of Structural Engineering, 128(2), 214-223.

[35]Cantero, D., OBrien, E. J., González, A., Enright, B., & Rowley, C. (2009). Highway bridge assessment for dynamic interaction with critical vehicles.

[36]Deng, L., He, W., & Shao, Y. (2015). Dynamic impact factors for shear and bending moment of simply supported and continuous concrete girder bridges. Journal of Bridge Engineering, 20(11), 04015005.

[37]Ding, L., Hao, H., Xia, Y., & Deeks, A. J. (2012). Evaluation of bridge load carrying capacity using updated finite element model and nonlinear analysis. Advances in structural engineering, 15(10), 1739-1750.

[38]McGetrick, P., Kim, C.-W., González, A., & O'Brien, E. J. (2012). Dynamic axle force and road profile identification using a moving vehicle. Paper presented at the The 25th KKCNN Symposium on Civil Engineering, Busan, Korea, 22-24 October, 2012.

[39]González, A. (2010). Vehicle-bridge dynamic interaction using finite element modelling *Finite element analysis*: InTech.

[40]Wolfert, A., Dieterman, H., & Metrikine, A. (1998). Stability of vibrations of two oscillators moving uniformly along a beam on a viscoelastic foundation. Journal of sound and vibration, 211(5), 829-842.

[41]Zhu, X., & Law, S.-S. (2016). Recent developments in inverse problems of vehicle–bridge interaction dynamics. Journal of Civil Structural Health Monitoring, 6(1), 107-128.

[42]Kalyankar, R., & Uddin, N. (2016). Simulating the effects of surface roughness on reinforced concrete T beam bridge under single and multiple vehicles. Advances in Acoustics and Vibration, 2016.

[43]Dodds, C., & Robson, J. (1973). The description of road surface roughness. Journal of sound and vibration, 31(2), 175-183.

[44]Green, M., & Cebon, D. (1997). Dynamic interaction between heavy vehicles and highway bridges. Computers & structures, 62(2), 253-264.

[45]Wang, T.-L., Huang, D., & Shahawy, M. (1992). Dynamic response of multigirder bridges. Journal of Structural Engineering, 118(8), 2222-2238.

[46]Henchi, K., Fafard, M., Talbot, M., & Dhatt, G. (1998). An efficient algorithm for dynamic analysis of bridges under moving vehicles using a coupled modal and physical components approach. Journal of sound and vibration, 212(4), 663-683.

[47]Kim, C. W., Kawatani, M., & Kim, K. B. (2005). Three-dimensional dynamic analysis for bridge–vehicle interaction with roadway roughness. Computers & structures, 83(19-20), 1627-1645.

[48]Deng, L., Wang, F., & He, W. (2015). Dynamic impact factors for simply-supported bridges due to vehicle braking. Advances in structural engineering, 18(6), 791-801.

[49]Moses, F. (1979). Weigh-in-motion system using instrumented bridges. Journal of transportation engineering, 105(3).

[50]O'Brien, E. J., Znidaric, A., & Dempsey, A. T. (1999). Comparison of two independently developed bridge weigh-in-motion systems. International Journal of Heavy Vehicle Systems, 6(1), 147-161.

[51]Ojio, T., & Yamada, K. (2002). Bridge weigh-in-motion systems using stringers of plate girder bridges. Paper presented at the Third International Conference on Weigh-in-Motion (ICWIM3) Iowa State University, Ames.

[52]BridgeMon. http://bridgemon.zag.si/.

[53]Chen, Y., Feng, M. Q., & Tan, C. A. (2006). Modeling of traffic excitation for system identification of bridge structures. Computer‐Aided Civil and Infrastructure Engineering, 21(1), 57-66.

[54]Ditlevsen, O., & Madsen, H. O. (1994). Stochastic vehicle-queue-load model for large bridges. Journal of Engineering Mechanics, 120(9), 1829-1847.

[55]Nowak, A. S. (1994). Load model for bridge design code. Canadian Journal of Civil Engineering, 21(1), 36-49.

[56]Enright, B., & O'Brien, E. J. (2013). Monte Carlo simulation of extreme traffic loading on short and medium span bridges. Structure and Infrastructure Engineering, 9(12), 1267-1282.

[57]OBrien, E. J., & Enright, B. (2011). Modeling same-direction two-lane traffic for bridge loading. Structural safety, 33(4-5), 296-304.

[58]Caprani, C. C., González, A., Rattigan, P. H., & OBrien, E. J. (2012). Assessment dynamic ratio for traffic loading on highway bridges. Structure and Infrastructure Engineering, 8(3), 295-304.

[59]Chen, S., & Wu, J. (2009). Dynamic performance simulation of long-span bridge under combined loads of stochastic traffic and wind. Journal of Bridge Engineering, 15(3), 219-230.

[60]Chen, S., & Wu, J. (2011). Modeling stochastic live load for long-span bridge based on microscopic traffic flow simulation. Computers & structures, 89(9-10), 813-824.

[61]Ministry of Land, I., Transport and Tourism (1970). Technical standard. Article 4: Design vehicles. Retrieved from http://www.mlit.go.jp/road/road_e/r1_standard.html

[62]Suzuki, M., Jinno, K., Tashiro, Y., Katsumata, Y., Liao, C., Nagayama, T., et al. (2016). Development and field experiment of routing-free multi-hop wireless sensor network for structural monitoring. Proc. ICSIC, 179-184.

[63]Agostinacchio, M., Ciampa, D., & Olita, S. (2014). The vibrations induced by surface irregularities in road pavements–a Matlab® approach. European Transport Research Review, 6(3), 267-275.

[64]Gao, W., Zhang, N., & Dai, J. (2008). A stochastic quarter-car model for dynamic analysis of vehicles with uncertain parameters. Vehicle system dynamics, 46(12), 1159-1169.

[65]Cebon, D. (1999). Handbook of vehicle-road interaction.

[66]Sun, L., & Kennedy, T. W. (2002). Spectral analysis and parametric study of stochastic pavement loads. Journal of Engineering Mechanics, 128(3), 318-327.

[67]Sayers, M. W. (1995). On the calculation of international roughness index from longitudinal road profile. Transportation Research Record(1501).

[68]Kropáč, O., & Múčka, P. (2009). Effects of longitudinal road waviness on vehicle vibration response. Vehicle system dynamics, 47(2), 135-153.

[69]Johannesson, P., Podgórski, K., & Rychlik, I. (2014). Modelling roughness of road profiles on parallel tracks using roughness indicators: Department of Mathematical Sciences, Division of Mathematical Statistics ….

[70]Liu, C., Wang, T.-L., & Huang, D. (2001). Impact study for multi-girder bridge based on correlated road roughness. Structural Engineering and Mechanics, 11(3), 259-272.

[71]Oliva, J., Goicolea, J. M., Antolín, P., & Astiz, M. Á. (2013). Relevance of a complete road surface description in vehicle–bridge interaction dynamics. Engineering Structures, 56, 466-476.

APPENDIX: DYNAMIC VEHICULAR FORCE EXPERIMENT

Vehicle bridge interaction is not only related with pavement design but also depends on vehicle characteristics and velocity. When a vehicle passes through the bridge with different speeds, the contact force between vehicle and bridge is altered, causing random dynamic response on bridge. In this research, a tire force experiment is conducted to find the relationship between shape profile of dynamic axle force with vehicle s and with the effect of vehicle hump. The sensor system includes: (1) a dynamic force sensor, (2) data processing system, (3) 5-centimeter hump, and (4) test vehicles. The PCB's quartz, piezoelectric dynamic force sensor with sensitivity of 0.2248 mV per Newton and 2000 Hz sampling frequency is the main measurement tool (Table 6.1). A 3-ton truck and a passenger car were used as the test vehicles of the experiment. Fig. 6.1 shows the sensor experiment setting and devices in dynamic tire force experiment. The experiment **is** implemented in Yokohama national University Campus on January 16th, 2018

(a) Force sensor

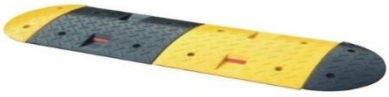

(b) Hump

(a) Data processign system

(d) Truck

Figure 6.1 : Experiment equipment and setting

Table 6.1: Force sensor specification

Parameters	Value
Measurement range (compression)	22.24 kN
Sensitivity	224.8 mV/kN
Max static force (compression)	35.59 kN
Broadband resolution	0.4448 N-rms
Frequency limit	0.0003 Hz – 75 kHz
Discharge time constant	≥ 2000 secs
Temperature range	-54 to 121 ^{o}C
Stiffness	1.9 kN/ μm
Weight	14 gm
Size (in mm)	16.51 x 9.14 x 12.7
Mounting	10-32 thread

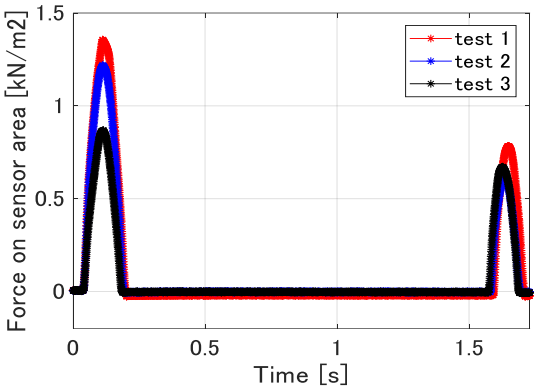

(b) Force at crawl speed

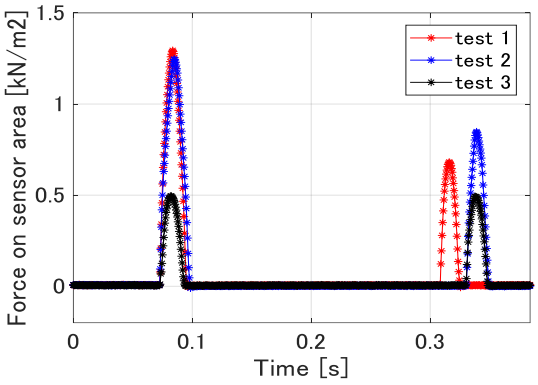

(b) Force at 40 km/h vehicle speed

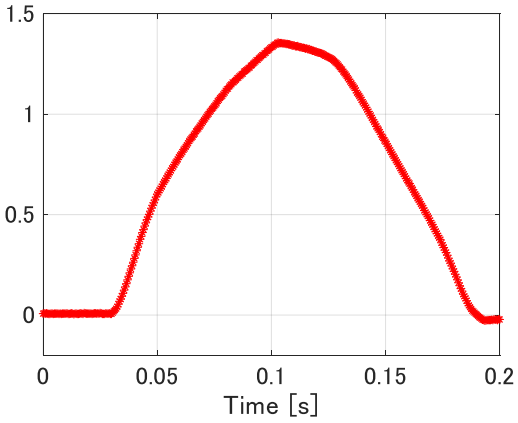

(c) Zoom-in force at crawl speed

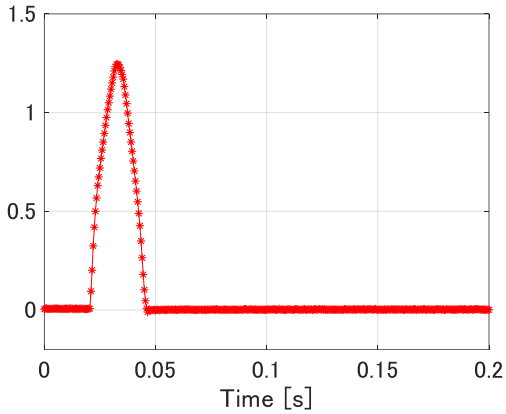

(d) Zoom-in force at 40 km/h vehicle speeds

Figure 6.2: Dynamic tire force profile of light truck in different speeds

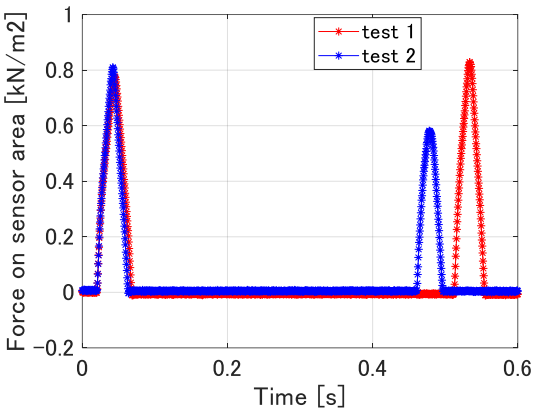

(a) Force without hummp

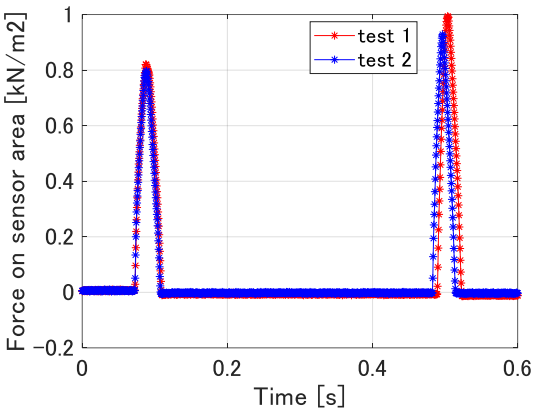

(b) Force with hump

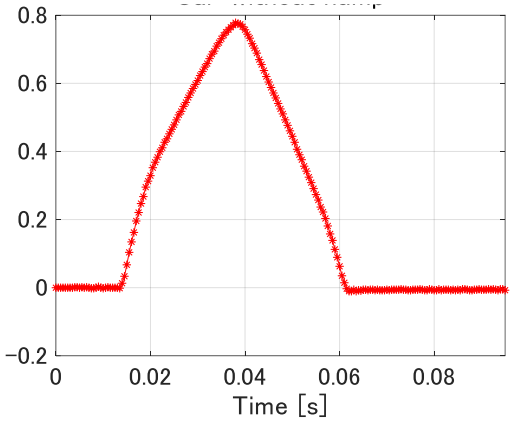

(c) Zoom-in force wihtout hump

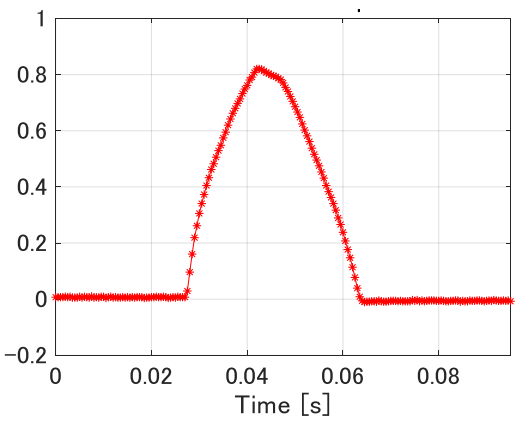

(d) Zoom-in force with hump

Figure 6.3: Dynamic tire force profile of paasenger car with and without hump (V=20 km/h)

In this experiment, the dynamic tire force of vehicle is measured under good surface condition and 5- centimetre hump with crawl, 20 km/h and 40 km/h velocity, respectively. To get the repeatability of experiment, each case is implemented for 3 runs. The variation of force profile at crawl speed and at 40 km/h speed is presented in Fig. 6.2. The result shows that the tire force profile is reduced as the vehicles pass through the sensor with higher speed. Fig. 6.3 shows the effect of hump in dynamic vehicular tire force at the same velocity of 20 km/h. Tables 6.1 and 6.2 show the variation of mean and standard deviation of dynamic force profile in second under effect of speed and hump. From the result of experiment, we could conclude that the impact tire force of vehicle wheel is significantly influenced by the changing of vehicle speed and roughness condition. The shape of impact tire force is in triangular or sine/cosine function with shape width reduce at higher speed and roughness. These results of experiment will be used for building the dynamic forcing function of time history analysis in next section of the research.

Table 6.2: Mean and standard deviation of dynamic tire forces due to speed (in second)

Case	Front wheel		Rear wheel	
	Mean	Standard deviation	Mean	Standard deviation
Crawl speed	0.152	0.009	0.118	0.002
20 km/h	0.048	0.009	0.037	0.003
40 km/h	0.0 28	0.002	0.024	0.004

Table 6.3: Mean and standard deviation of dynamic tire forces due to hump (in second)

Case	Front wheel		Rear wheel	
	Mean	Standard deviation	Mean	Standard deviation
Wihtout hump	0.047	0.002	0.04	0.005
With hump	0.048	0.009	0.037	0.003